

Nitrous oxide emissions from variable rate application of nitrogen fertilizer to *Panicum virgatum*  
L. in Québec, Canada.

Alexia M. Bertholon

Department of Natural Resource Sciences

McGill University, Montreal

November 2021

A thesis submitted to McGill University in partial fulfillment  
of the requirements of the degree of  
MASTER OF SCIENCE

© Alexia M. Bertholon, 2021

## Table of Contents

List of Tables.....	v
List of Figures.....	vi
List of Symbols and Abbreviations.....	ix
Abstract.....	x
Résumé.....	xii
Acknowledgements.....	xiv
Contribution of Authors.....	xvi
General Introduction.....	1
Chapter 1: Literature review.....	3
1.1 Agriculture and greenhouse gas emissions.....	3
1.2 Microorganisms and nutrient cycling.....	3
1.2.1 Mineralization.....	5
1.2.2 Ammonia oxidation and nitrification.....	5
1.2.3 Nitrifier denitrification.....	6
1.2.4 Biological denitrification.....	8
1.2.5 Respiration resulting from carbon metabolism and consequences for N <sub>2</sub> O production.....	9

1.3 Factors contributing to the variation in CO <sub>2</sub> and N <sub>2</sub> O fluxes from soil-plant systems.....	10
1.3.1 Topography and soil type.....	11
1.3.2 Soil temperature.....	11
1.3.3 Soil moisture.....	12
1.3.4 Soil pH.....	12
1.4 Conclusions and future directions.....	13
Chapter 2: Management zone identification from soil properties and spectral images in a switchgrass field.....	15
Abstract.....	16
2.1 Introduction.....	17
2.2 Materials and methods.....	20
2.2.1 Site description.....	20
2.2.2 Soil sampling and physicochemical analysis.....	20
2.2.3 Apparent soil electrical conductivity and multispectral measurements.....	23
2.2.4 Geostatistical analysis of soil physicochemical properties.....	23
2.2.5 Management zone delineation.....	24
2.2.6 Comparing alternative maps to the Reference map.....	26
2.3 Results.....	26

2.3.1 Spatial autocorrelation of soil physicochemical properties.....	26
2.3.2 Management zones.....	29
2.4 Discussion.....	34
2.4.1 Site-specific management zone delineation.....	34
2.4.2 Management Zone Analyst, a practical tool to make maps from proximal soil sensing data.....	36
2.5 Conclusion.....	38
2.6 References.....	40
Connecting Paragraph.....	45
Chapter 3: Variable rate nitrogen fertilizer application induces hot moments in nitrous oxide emissions in a switchgrass field in Southern Québec, Canada.....	46
Abstract.....	47
3.1 Introduction.....	47
3.2 Materials and Methods.....	50
3.2.1 Site description.....	50
3.2.2 Experimental design.....	50
3.2.3 Gas sampling and analysis.....	50
3.2.4 Gas flux calculations and seasonal emissions.....	52

3.2.5 Ancillary measurements.....	54
3.2.6 Soil sampling and analysis.....	54
3.2.7 Plant sampling and analysis during the growing season.....	55
3.2.8 Statistical analysis.....	57
3.3 Results.....	57
3.3.1 Gas emissions.....	57
3.3.2 Biomass and ancillary measurements.....	66
3.4 Discussion.....	71
3.4.1 Gas emissions and site-specific N.....	71
3.4.2 Ancillary measurements and management zones.....	72
3.5 Conclusions.....	73
3.6 References.....	74
General Discussion.....	76
General Conclusions.....	81
References.....	83

## List of Tables

<b>Table 2-1.</b> Soil physicochemical properties (0–20 cm) in an 8.9 ha switchgrass field in southern Québec, Canada. Data are from 128 soil samples collected in May 2017.....	22
<b>Table 2-2.</b> Parameters used to delineate map boundaries with Management Zone Analyst software.....	26
<b>Table 2-3.</b> Descriptive statistics for selected physicochemical properties, apparent electrical conductivity and coarse elevation in Zones 1, 2 and 3 of the ‘Simple’ map of an 8.9 ha switchgrass field in southern Québec, Canada. The ‘Simple’ map is illustrated in Fig. 2-6.....	34
<b>Table 3-1.</b> Cumulative growing season emissions in 2018, presented as the interpolated cumulative values $\pm$ SEM, n=24.....	64
<b>Table 3-2.</b> Cumulative growing season emissions in 2019, presented as the interpolated cumulative values $\pm$ SEM, n=24.....	65
<b>Table 3-3.</b> Linear regression of cumulative growing season emissions, in relation to the N fertilizer rate. The slope and intercept of the best-fit line ( $\pm$ SEM) were calculated with R statistical software.....	66
<b>Table 3-4.</b> End of season above ground biomass yield (t dry matter ha <sup>-1</sup> ) adjacent to the gas sampling locations. Values are the mean $\pm$ SEM, n=3.....	71

## List of Figures

<b>Figure 1-1.</b> Major N <sub>2</sub> O emission pathways in soil. Adapted from Kool et al. (2011).....	5
<b>Figure 2-1.</b> Soil sampling locations in an 8.9 ha switchgrass field in southern Québec, Canada. The sampling pattern was a random within grid sampling design. The map was drawn in ArcMap (version 10.4.1) and the bare soil image was taken from Google Earth Pro (version 7.3.2.5776).....	21
<b>Figure 2-2.</b> Total sand content, determined by geostatistical interpolation, in an 8.9 ha switchgrass field in southern Québec, Canada.....	28
<b>Figure 2-3.</b> Soil pH determined by geostatistical interpolation, in an 8.9 ha switchgrass field in southern Québec, Canada.....	29
<b>Figure 2-4.</b> Reference map of an 8.9 ha switchgrass field in southern Québec, Canada. The map was drawn from 10 variables, including 8 soil physicochemical properties (C:N ratio, the total sand, silt and clay content, extractable phosphorous concentration, total carbon concentration, soil moisture content and pH) along with coarse elevation and apparent soil electrical conductivity (ECa 1.5 m), with Management Zone Analyst.....	30
<b>Figure 2-5.</b> ECa based map of the 8.9 ha switchgrass field in southern Québec, Canada. The map was drawn from the coarse elevation and apparent soil electrical conductivity (ECa 1.5 m and ECa 0.75 m) data with Management Zone Analyst.....	31
<b>Figure 2-6.</b> Simple map of the 8.9 ha switchgrass field in southern Québec, Canada. The map was drawn from the coarse elevation, apparent soil electrical conductivity (ECa 1.5 m and ECa 0.75 m) and the multispectral red, green and blue images of the bare soil surface with Management Zone Analyst.....	32

**Figure 2-7.** Texture map of the 8.9 ha switchgrass field in southern Québec, Canada, based on sand, silt and clay content, drawn with Management Zone Analyst.....33

**Figure 3-1.** Map of the experimental switchgrass field, showing the treatment blocks and location of biomass and soil sampling points.....56

**Figure 3-2.** Weather data for the A: 2018 sampling season. Total daily precipitation (mm) is represented by black bars. Average daily temperature (°C) is represented by the black line. Mean CO<sub>2</sub> flux time series in B: Zone 1 and C: Zone 3 on every sampling day during the 2018 sampling season. Error bars are ±SEM (n=3). The N fertilizer was applied on Julian day 151 (May 31, 2018), indicated by the black arrow.....59

**Figure 3-3.** Weather data for the A: 2018 sampling season. Total daily precipitation (mm) is represented by black bars. Average daily temperature (°C) is represented by the black line. Mean N<sub>2</sub>O flux time series in B: Zone 1 and C: Zone 3 on every sampling day during the 2018 sampling season. Error bars are ±SEM (n=3). The N fertilizer was applied on Julian day 151 (May 31, 2018), indicated by the black arrow.....60

**Figure 3-4.** Weather data for the A: 2019 sampling seasons. Total daily precipitation (mm) is represented by black bars. Average daily temperature (°C) is represented by black line. Mean CO<sub>2</sub> flux time series in B: Zone 1 and C: Zone 3 on every sampling day during the 2019 sampling season. Error bars are ±SEM (n=3). The N fertilizer was applied on Julian day 169 (June 18, 2019), indicated by the black arrow.....61

**Figure 3-5.** Weather data for the A: 2019 sampling seasons. Total daily precipitation (mm) is represented by black bars. Average daily temperature (°C) is represented by the black line. Mean N<sub>2</sub>O flux time series in B: Zone 1 and C: Zone 3 on every sampling day during the 2019

sampling season. Error bars are  $\pm$ SEM (n=3). The N fertilizer was applied on Julian day 169 (June 18, 2019), indicated by the black arrow.....62

**Figure 3-6.** Cumulative seasonal emissions of A: CO<sub>2</sub> and B: N<sub>2</sub>O from switchgrass plots in the 2018 and 2019 seasons. Points are the average of n=3 measurements per zone, and error bars are  $\pm$ SEM.....63

**Figure 3-7.** Average soil NH<sub>4</sub><sup>+</sup> and NO<sub>3</sub><sup>-</sup> concentrations for each fertilizer application rate in 2018 of A: Zone 1 NO<sub>3</sub><sup>-</sup>, B: Zone 3 NO<sub>3</sub><sup>-</sup>, C: Zone 1 NH<sub>4</sub><sup>+</sup>, D: Zone 3 NH<sub>4</sub><sup>+</sup>. Fertilizer applied on 151 (May 31, 2018). Points are the mean (n=3) with  $\pm$ SEM bars.....67

**Figure 3-8.** Average soil NH<sub>4</sub><sup>+</sup> and NO<sub>3</sub><sup>-</sup> concentrations for each fertilizer application rate in 2019 of A: Zone 1 NO<sub>3</sub><sup>-</sup>, B: Zone 3 NO<sub>3</sub><sup>-</sup>, C: Zone 1 NH<sub>4</sub><sup>+</sup>, D: Zone 3 NH<sub>4</sub><sup>+</sup>. Fertilizer applied on 169 (June 18, 2019). Points are the mean (n=3) with  $\pm$ SEM bars.....68

**Figure 3-9.** Average N concentration in switchgrass biomass in A: Zone 1 and B: Zone 3 during the 2018 sampling season. The N fertilizer was applied on Julian day 151 (May 31, 2018). Points are the mean (n=3) with  $\pm$ SEM bars.....69

**Figure 3-10.** Average N concentration in switchgrass biomass in A: Zone 1 and B: Zone 3 during the 2019 sampling season. The N fertilizer was applied on Julian day 169 (June 18, 2019). Points are the mean (n=3) with  $\pm$ SEM bars.....70

## **List of Symbols and Abbreviations**

CO<sub>2</sub> Carbon dioxide

CH<sub>4</sub> Methane

GHG Greenhouse gas

N Nitrogen

N<sub>2</sub> Nitrogen gas

NH<sub>3</sub><sup>-</sup> Ammonia

NH<sub>4</sub><sup>+</sup> Ammonium

NO Nitric oxide

N<sub>2</sub>O Nitrous oxide

NO<sub>2</sub><sup>-</sup> Nitrite

NO<sub>3</sub><sup>-</sup> Nitrate

SEM Standard error of mean

## Abstract

Nitrogen (N) fertilizer is essential to maintain agricultural yields but is susceptible to reactions that produce nitrous oxide (N<sub>2</sub>O), which acts as a greenhouse gas and contributes to stratospheric ozone depletion. It is difficult to predict where these reactions will produce ‘hot spots’ of high N<sub>2</sub>O fluxes in a field, as well as the ‘hot moments’ when peak N<sub>2</sub>O fluxes occur. The objective of this study is to relate the N<sub>2</sub>O fluxes in a *Panicum virgatum* L. (switchgrass) field to N fertilizer application rates of 0, 50, 100, and 150 kg N ha<sup>-1</sup> while considering the spatial-temporal heterogeneity of the field. In summer 2017, soil samples were collected at 128 locations in an 8.87 ha switchgrass field in the Cookshire-Eaton region (45°20'N, 71°46'W) of Québec, Canada. The sandy loam soil was analysed for standard soil test parameters: macro- and micro-nutrient content, pH and texture. In addition, proximal soil sensing was done to characterize the elevation, electrical conductivity and surface spectral reflectance. This data was used to generate a spatial soil map of the field with R 3.4.1 statistical software and ArcGIS, which revealed three distinct management zones in the field. In spring 2018, four N fertilizer rates were applied to blocks (15 m wide x 100 m long), which created four blocks with variable N fertilizer rates in the high-yielding switchgrass zone and four blocks with variable N fertilizer rates in the low-yielding switchgrass zone. Non-flow-through non-steady-state chambers were installed (n=3 per block) for manual gas sampling and N<sub>2</sub>O fluxes were calculated during a 1 h period every 7-10 d during the growing season. The experiment was repeated in spring 2019 in the same management zones but in newly-selected blocks that had uniform fertilization in the 2018 growing season. Four N fertilizer rates were applied at random to 4 blocks in the high-yielding zone, plus 4 blocks in the low-yielding zone, and gas sampling chambers (n=3) were placed in new locations in each block. The “hot moments” of N<sub>2</sub>O flux occurred in the first 30 d

after N fertilizer application. Although N<sub>2</sub>O fluxes differed in the management zones in 2018, there were no distinctive “hot spots” in the switchgrass field in the 2019 growing season. However, the cumulative N<sub>2</sub>O emission in each growing season tended to increase with greater N fertilizer rates, suggesting that applying more N fertilizer increased the risk of gaseous N loss, probably through denitrification. I conclude that precision agriculture techniques based on geospatial characterization of agricultural fields may help to calibrate site-specific N fertilizer inputs and meet agroenvironmental goals by improving crop production while reducing N<sub>2</sub>O emissions.

## Résumé

L'engrais azoté (N) est essentiel pour maintenir les rendements agricoles, mais il est susceptible de produire de l'oxyde nitreux (N<sub>2</sub>O), qui agit comme un gaz à effet de serre et contribue à l'appauvrissement de l'ozone stratosphérique. Il est difficile de prédire où ces réactions produiront des « points chauds » de flux élevés de N<sub>2</sub>O dans un champ, ainsi que les « moments chauds » de flux élevés de N<sub>2</sub>O. L'objectif de cette étude est de relier les flux de N<sub>2</sub>O dans un champ de *Panicum virgatum* L. (panic érigé) aux taux d'épandage d'engrais azoté de 0, 50, 100 et 150 kg N ha<sup>-1</sup>, tout en considérant l'hétérogénéité spatio-temporelle du champ. Durant l'été 2017, des échantillons de sol ont été prélevés à 128 emplacements dans un champ de panic érigé de 8,87 ha dans la région de Cookshire-Eaton (45°20'N, 71°46'O), Québec, Canada. Le sol, un loam sablonneux, a été analysé pour les propriétés suivantes : la teneur en macro et micronutriments, la conductivité électrique, le pH et la composition de la texture du sol. La réflectance spectrale de la surface ainsi qu'une détection proximale du sol mesurant l'altitude et la conductivité électrique ont été utilisés pour générer une carte de sol avec le logiciel statistique R 3.4.1 et ArcGIS. Cette caractérisation a révélé trois zones de gestion distinctes dans le champ. Au printemps 2018, chaque dose d'N a été appliquée aux blocs (15 m de largeur par 100 m de longueur), ce qui a créé quatre blocs avec des doses d'N variables dans la zone de panic érigé à haut rendement et quatre blocs avec des doses d'N variables dans la zone à faible rendement. Des chambres de gaz ont été installées (n = 3 par bloc) pour l'échantillonnage manuel des gaz et les flux de N<sub>2</sub>O ont été calculés pendant une période de 1 h tous les 7 à 10 jours pendant la saison de croissance. L'expérience a été répétée au printemps 2019 dans les mêmes zones de gestion mais dans des blocs nouvellement sélectionnés qui avaient une fertilisation uniforme au cours de la saison de croissance 2018. Quatre taux d'engrais azoté ont été appliqués au hasard à 4

blocs dans la zone à haut rendement, et 4 blocs dans la zone à faible rendement. Des chambres d'échantillonnage de gaz (n=3) ont été placées à de nouveaux emplacements dans chaque bloc. Les « moments chauds » du flux de N<sub>2</sub>O se sont produits dans les 30 premiers jours après l'application d'engrais N. Même s'il y avait des différences entre les flux de N<sub>2</sub>O dans les zones de gestion en 2018, il n'y avait pas de « points chauds » distinctifs dans le champ de panic érigé au cours de la saison de croissance en 2019. Cependant, les émissions cumulées de N<sub>2</sub>O à chaque saison de croissance avaient tendance à augmenter avec des taux d'engrais N plus élevés, ce qui suggère dose plus élevée d'engrais azoté augmentait le risque de perte de N gazeux, probablement par dénitrification. En conclusion, les techniques d'agriculture de précision basées sur la caractérisation géospatiale des champs agricoles peuvent aider à calibrer les apports d'engrais azoté spécifiques au site et à atteindre les objectifs agroenvironnementaux en améliorant la production agricole tout en réduisant les émissions de N<sub>2</sub>O.

## **Acknowledgements**

First and foremost, I would like to express my deep gratitude to my supervisor Dr. Joann K. Whalen and co-supervisor Dr. Louis Longchamps, for their continued expertise and guidance. I could write a book about all that I learned from Dr. Joann K. Whalen. Her weekly lab meetings were incredibly helpful for developing my academic and professional skills. She worked diligently to review my writing and gave extremely detailed feedback, which helped me think more clearly about my research. Many thanks are owed to Dr. Louis Longchamps who was key to the successful execution of my field research. His guidance related to all things precision agriculture helped me develop skills required for better understanding the agriculture of today and tomorrow.

I would like to thank all the students and staff of the Soil Ecology Research Group at McGill University for their support and aid in my growth and understanding of the soil science world. A very special thanks is due to Hicham Benslim, Chih-Yu Huang, Yawen Shen and Nasser Hussain for helping me analyse my thousands of GHG samples with the GC and better understand GHG analysis. I am extremely grateful for the department of Natural Resource Sciences within the Faculty of Agricultural and Environmental Sciences at McGill University for supporting my studies via funding by the Graduate Excellence Award.

I would like to thank the students and staff of Agriculture & Agri-Food Canada. A special thanks to Éléonore Tremblay, Philippe Vigneault, Gaston Mercier, Gilles St-Laurent, Sarah-Maude Parent, Edith Fallon, Élianne Ricard, Andrée-Dominique Baillargeon, and Camille Charbonneau. I would especially like to thank Dr. Athyna N. Cambouris for her assistance

throughout the project by helping plan the field design, sending students to help me with the collection of field data, analysing the soil and plant samples.

Last but not least, a special thanks is deserved to my family. My studies would not be possible without the unconditional support from my sister, Chloé, parents, Gerard and Elizabeth, and grandparents, Tom, Mickey, Pierre and Janine, who taught me the importance of education for a meaningful life.

## Contribution of Authors

My thesis consists of a general literature review followed by two experimental chapters. My thesis includes the thesis components required for a manuscript-based style, according to the guidelines provided by the Office of Graduate and Postdoctoral Studies of McGill University.

Chapter 1 is a literature review that covers the existing literature related to my study with a focus on field variability and important factors contributing to greenhouse gas emissions. An overview of my objectives is provided at the end of this chapter.

Chapter 2 consists of an experiment completed to address my first objectives regarding field variability. A connecting paragraph is provided after Chapter 2 to connect the work completed in Chapter 2 to the objectives of Chapter 3. Chapter 3 uses information from Chapter 2 to address the questions related to my objectives on the topic of greenhouse gases.

Chapter 1 was written by the candidate, Alexia M. Bertholon, and edited by her supervisors Dr. Joann K. Whalen and Dr. Louis Longchamps. Chapter 2 was authored by the candidate and edited by her supervisor Dr. Joann K. Whalen, co-supervisor Dr. Louis Longchamps and Dr. Athyna Cambouris. Chapter 2 is in preparation for submission as a special issue paper to the international journal *Crop and Pasture Science*. Chapter 3 was written by the candidate and revised by her supervisors Dr. Joann K. Whalen and Dr. Louis Longchamps.

The field experiment was designed the candidate, Alexia M. Bertholon, in collaboration with Dr. Louis Longchamps, Dr. Athyna N. Cambouris, Dr. Pierre Dutilleul and Dr. Joann K. Whalen. The candidate was responsible for the collection and processing of field data, with the help of AAFC staff. Laboratory analysis of the soil data for Chapter 2 was provided by the research group of Dr. Athyna N. Cambouris. The data interpretation and thesis manuscript

preparation was the responsibility of the candidate under the supervision of Dr. Joann K. Whalen and Dr. Louis Longchamps.

## General Introduction

Global climate warming is the result of a surplus of greenhouse gases in the atmosphere that trap heat radiating from Earth towards space. Nitrous oxide ( $\text{N}_2\text{O}$ ) is a potent greenhouse gas with a half-life of 120 years and almost 300 times the global warming potential of carbon dioxide ( $\text{CO}_2$ ) (de Carvalho et al., 2017). Agriculture accounts for approximately 70% of all anthropogenic  $\text{N}_2\text{O}$  emissions, primarily due to inefficient uptake of nitrogen (N) fertilizer by crops (Wile et al., 2014). Denitrification is a major biological process that produces  $\text{N}_2\text{O}$  emitted from the agricultural sector and is modulated by the availability of substrates (e.g., nitrate and available organic carbon) and edaphic factors such as temperature, oxygen concentration and pH, which result in variable denitrification rates through the soil profile (Munch & Velthof, 2007). Since human management of agricultural land alters substrate availability and edaphic factors, it is important to select management practices that will not trigger the denitrification process.

Managing the nitrogen fertilizer inputs to agricultural fields is the most practical way to constrain denitrification and reduce  $\text{N}_2\text{O}$  emissions. In North America, mineral fertilizer represents 48-55% of the N applied for crop production (Liu et al., 2010). Conventional fertilization practices apply a uniform fertilizer rate across fields, without regard for the underlying heterogeneity in soil properties. An average N fertilizer rate will deliver too much, too little or just enough N fertilizer for different parts of the field. When N fertilizer rates are in excess of crop requirements, this may trigger denitrification and cause  $\text{NO}_3^-$  loss via leaching, while reducing the net profit because N fertilizer lost from the field cannot support crop growth. When crops receive insufficient N fertilizer, they will produce less yield and less revenue for the agricultural producer. Precision agriculture is a method developed to avoid inefficient fertilization practices that uses spatial data to calculate site-specific N fertilizer rates within a

heterogeneous field. I hypothesize that site-specific N fertilizer rates will reduce the N<sub>2</sub>O emissions of a field, compared to applying a uniform N fertilizer rate on the field.

The global objective of my M.Sc. thesis project is to understand how soil spatial variability influences the microbially-mediated processes that produce N<sub>2</sub>O and determine if adjusting the N fertilizer rate according to the principles of precision agriculture will lower N<sub>2</sub>O emissions. My general objectives were 1) to describe the site-specific variability of a heterogeneous agricultural field under switchgrass (*Panicum virgatum* L.) production, and determine whether a limited number of proximal soil variables could be as effective as conventional soil test data in distinguishing the field management zones, and 2) to compare N<sub>2</sub>O fluxes from four N fertilizer rates, and in relationship to auxiliary measurements of spatio-temporal variability, and 3) to quantify the switchgrass yield relative to N fertilizer application and N<sub>2</sub>O fluxes within each field management zone. This will allow me to understand how management zones influence the temporal pattern of N<sub>2</sub>O flux and determine if precision agriculture techniques could lower the N losses from N<sub>2</sub>O emissions in one field under switchgrass production in Québec.

## **Chapter 1: Literature review**

### **1.1 Agriculture and greenhouse gas emissions**

Rising methane (CH<sub>4</sub>), carbon dioxide (CO<sub>2</sub>) and nitrous oxide (N<sub>2</sub>O) concentrations in the atmosphere act as greenhouse gases (GHG) that trap radiative energy, thereby affecting the global climate and altering weather patterns. Globally, agricultural activities are responsible for ~5.0–5.8 Gt CO<sub>2</sub>-eq yr<sup>-1</sup> or ~11% of anthropogenic CO<sub>2</sub>, CH<sub>4</sub> and N<sub>2</sub>O emitted into the atmosphere. There is particular concern about the agricultural sources of N<sub>2</sub>O, which is a potent ozone-depleting substance. The agricultural sector produced about 2 Gt CO<sub>2</sub>-eq yr<sup>-1</sup> of N<sub>2</sub>O in 2010 and is expected to reach more than 4 Gt CO<sub>2</sub>-eq yr<sup>-1</sup> by 2100 (Gernaat et al., 2015; Frank et al., 2018). We need to reduce the N<sub>2</sub>O emissions and the N<sub>2</sub>O concentration in the atmosphere because its global warming potential is approximately 300 times more than CO<sub>2</sub> and it is a persistent GHG with a half-life of more than 100 years (Munch & Velthof, 2007).

Agricultural soils are a major global source of N<sub>2</sub>O and other GHG because they receive fertilizer, are irrigated and are cultivated regularly. All of these activities stimulate the biological (microbially-mediated) reactions that generate GHG. Improved agricultural management such as site-specific N fertilizer application is expected to reduce N<sub>2</sub>O emissions. This literature review will discuss the soil microbial processes and soil characteristics that are responsible for the N<sub>2</sub>O emissions from agricultural soils.

### **1.2 Microorganisms and nutrient cycling**

The gaseous compound N<sub>2</sub>O, byproduct of microbial reactions in the N cycle, makes a major contribution to global climate change. The soil N cycle is mediated by soil

microorganisms, whose activities are responsible for virtually all of the N cycling reactions in soil (Wrage et al., 2018). When N fertilizers are added to agricultural soil, they are transformed through microbial processes. For example, urea, which accounts for approximately 60% of global N fertilizer application (Fisher et al., 2016), is solubilized in water and then hydrolyzed by the extracellular enzyme urease, which produced by microbial cells. Urea hydrolysis releases ammonium carbonate, an unstable compound that chemically decomposes into ammonia ( $\text{NH}_3$ ) and  $\text{CO}_2$  before reacting with  $\text{H}^+$  to produce ammonium ( $\text{NH}_4^+$ ) cation (Kiss & Simihăian, 2002). Although  $\text{NH}_4^+$  can be absorbed by crops, it may undergo other biological transformations in soil. For example,  $\text{NH}_4^+$  resulting from the hydrolysis of urea can be oxidized by soil bacteria and archaea to produce nitrate ( $\text{NO}_3^-$ ) (Fisher et al., 2016). Ammonium oxidation, nitrifier denitrification and denitrification are three major soil pathways that produce  $\text{N}_2\text{O}$  (Fig. 1-1). It is important to note that  $\text{N}_2\text{O}$  is generated in the nitrification (aerobic) and denitrification (anaerobic) reactions, either as a by-product or direct intermediate of the reaction. Therefore, there is always some  $\text{N}_2\text{O}$  flux from soil. The magnitude of the  $\text{N}_2\text{O}$  flux depends upon the availability of substrates and edaphic factors that govern microbial activity.

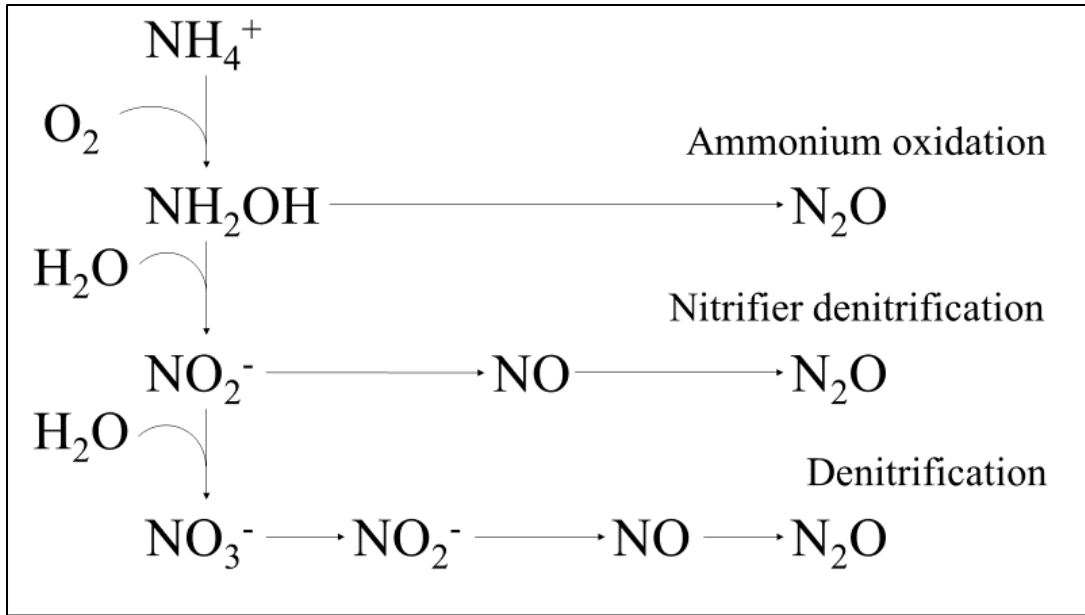


**Figure 1-1.** Major N<sub>2</sub>O emission pathways in soil. Adapted from Kool et al. (2011).

### 1.2.1 Mineralization

Mineralization is the enzyme-catalyzed transformation of organic N compounds into  $\text{NH}_4^+$  (Whalen & Sampedro, 2010). Urea, protein, and peptides are just a few examples of organic substances that undergo N mineralization through the hydrolysis of these compounds by urease, protease and peptidase enzymes. The  $\text{NH}_4^+$  released from mineralization is used directly by plants and microorganisms, or is transformed through the microbially-mediated reaction of ammonia oxidation, followed by nitrification reactions.

### 1.2.2 Ammonia oxidation and nitrification

Nitrification is a key process in the global N cycle. Nitrification, which transforms

ammonia ( $\text{NH}_3$ ) into the final product of nitrate ( $\text{NO}_3^-$ ), is an energy-generating reaction for many soil microorganisms, including bacteria and fungi (Hayatsu et al., 2008). The three-step reaction is mediated by ammonia oxidizing bacteria and nitrite oxidizing bacteria (Banning et al., 2015). Ammonia oxidation by ammonia oxidizing archaea and bacteria is the first, rate-limiting step of nitrification (Merbt et al., 2016). Ammonia oxidizing bacteria oxidize  $\text{NH}_3$  into hydroxylamine and subsequently to nitrite ( $\text{NO}_2^-$ ) with the ammonia monooxygenase and hydroxylamine oxidoreductase enzymes. Nitrous oxide is a byproduct of the ammonia oxidation reaction. Nitrite oxidizing bacteria then oxidize the  $\text{NO}_2^-$  into  $\text{NO}_3^-$  with nitrite oxidoreductase.

This reaction is initiated when ammonia oxidizing bacteria have ample substrate, i.e.,  $\text{NH}_3$ . In addition to  $\text{NH}_3$  derived from mineralization of decaying organic matter, N fertilizers such as urea are a source of  $\text{NH}_3$  for ammonia oxidizers. Furthermore, N fertilizers increase plant biomass, leading to more photosynthesis and more root exudation, a source of labile organic carbon that is readily metabolized by ammonia oxidizing archaea and bacteria, accelerating their growth and enzymatic processes, which include  $\text{N}_2\text{O}$  production. However, the application of N fertilizers is often associated with a significant increase in population sizes of the ammonia oxidizing bacteria, which are either better adapted or better competitors for N fertilizer inputs than the ammonia oxidizing archaea present within the soil (Cui et al., 2008; Xiang et al., 2017). Thus, most of the  $\text{N}_2\text{O}$  production in well-aerated agricultural soils is probably related to the activity of ammonia oxidizing bacteria.

### *1.2.3 Nitrifier denitrification*

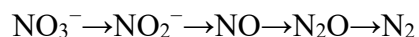
Ammonia-oxidizing bacteria also produce  $\text{N}_2\text{O}$  via nitrifier denitrification, which reduces  $\text{NO}_2$  into  $\text{N}_2\text{O}$  and  $\text{N}_2$  (Wrage-Mönnig et al., 2018). Nitrifier denitrification is catalyzed by nitrite

reductase and nitric oxide reductase (Shi et al., 2017). A study using the dual-isotope method, which can differentiate between four biological pathways for N<sub>2</sub>O production using <sup>15</sup>N and <sup>18</sup>O, found that nitrifier denitrification accounted for 39 and 65 % of N<sub>2</sub>O production in acidic and alkaline soils, respectively (Shi et al., 2017). Nitrifier denitrification occurs when oxygen levels are < 0.20 mg O<sub>2</sub> L<sup>-1</sup> (Li et al., 2018), which is common in microsites of well-drained agricultural soils within C-rich particles and aggregates (Seitzinger et al., 2006). More N<sub>2</sub>O was produced from nitrifier denitrification when water-filled pore space was 50-70 % than from biological denitrification, which is optimal at ≥80 % water-filled pore space (Kool et al., 2011). However, nitrifier denitrification depends upon the substrates supplied by ammonia-oxidizing bacteria, which is why ammonia-oxidizing bacteria that received NH<sub>4</sub><sup>+</sup> additions produced more N<sub>2</sub>O fluxes (Carey et al., 2016; Meinhardt et al., 2018). A laboratory experiment by Meinhardt et al. (2018) with control (0 μmol NH<sub>4</sub><sup>+</sup> g soil<sup>-1</sup>) and amended (40 μmol NH<sub>4</sub><sup>+</sup> g soil<sup>-1</sup>) soils that were saturated to ~60% water-filled pore space, ensuring conditions optimal for nitrifier denitrification, showed an increase in ammonia oxidizing population (based on *amoA* gene counts) from  $2.18 \times 10^6 \pm 3.29 \times 10^5$  to  $9.81 \times 10^7 \pm 2.70 \times 10^7$  g soil<sup>-1</sup> (P = 0.004) in the N amended soil and decreased in the control (P = 0.02). Furthermore, the activity of the ammonia-oxidizing bacteria increased 87-fold in the N-amended soil (*amoA* transcript abundance, P = 0.002). In a switchgrass field with plots of unfertilized and synthetic N amendments (9 μmol NH<sub>4</sub><sup>+</sup> g soil<sup>-1</sup> year<sup>-1</sup>), the ammonia-oxidizing bacteria *amoA* gene count increased with N amendment (P < 0.0001) and was correlated with N<sub>2</sub>O flux in the N amended (R<sup>2</sup> = 0.72, P < 0.0001) and unfertilized plots (R<sup>2</sup> = 0.51, P = 0.002; Meinhardt et al., 2018). Therefore, we should expect N<sub>2</sub>O flux from unsaturated soils due to the combined ammonia oxidation and

nitrifier denitrification processes, particularly when ammonium-based fertilizers are applied to agroecosystems.

#### 1.2.4 Biological denitrification

Biological denitrification, hereafter referred to as denitrification, is the sequential reduction of  $\text{NO}_3^-$  that produces  $\text{N}_2$  as a final product, with gaseous  $\text{NO}$  and  $\text{N}_2\text{O}$  as intermediate products of incomplete denitrification (Chen et al., 2008).



Biological denitrification is catalyzed by any soil microorganism (bacteria and fungi) that possesses the genes that encode for the reductive enzymes, such as *nirK* and *nirS* (functionally equivalent single-copy genes coding for nitrite reductases) and *nosZ* (nitric oxide reductase).

Denitrifiers require a minimum of 5 mg  $\text{kg}^{-1}$  soil  $\text{NO}_3^-$  N for this reaction (Conen et al., 2000). The reaction is optimal at pH 7.0 but is reported in soils with pH 5.0 to 9.0 (Scholefield et al., 1997). Soil biological processes, including denitrification, increase at higher soil temperatures, resulting in significantly more  $\text{N}_2\text{O}$  flux in a sandy loam pasture soil incubated at 20 °C and 25 °C were significantly higher than those incubated at 10 °C and 15 °C ( $P < 0.001$ , at 24 h of incubation), with cumulative denitrification responsible for the production of 235, 408, 1027 and 1525  $\mu\text{g N}_2\text{O-N kg}^{-1}$  soil, respectively (Abdalla et al., 2009). Biological denitrification always occurs under anaerobic soil conditions (Okiobe et al., 2019), meaning that the reaction is affected by soil moisture and the oxygen concentration. Therefore, the denitrification ‘hot moments’ of high  $\text{N}_2\text{O}$  flux from agricultural soils tend to occur in summer, when warmer soil

temperatures are recorded, and after rainfall events that create anaerobic conditions (temporarily) in the soil.

### *1.2.5 Respiration resulting from carbon metabolism and consequences for N<sub>2</sub>O production*

Soil organic matter is the largest terrestrial C pool, containing about 50% C, and responsible for the storage of approximately 1500 Pg C in the upper 1 m layer of soils worldwide (FAO & ITPS 2015). The C in soil originates from primary producers, which fix CO<sub>2</sub> from the atmosphere to produce sugars through photosynthesis. The main reaction in the Calvin cycle of photosynthesis that reduces CO<sub>2</sub> to sugar is the carboxylation of ribulose-1,5-biphosphate (Sharkey et al., 2012). This reaction is catalyzed by the Rubisco enzyme, which is present in plants, algae and many bacteria. Due to the high N requirement for Rubisco production (approximately 20% of total leaf protein is used for Rubisco), supplemental N fertilizer is required for non-leguminous agricultural plants, affecting the global N cycle (Sharkey et al., 2012). While most of the C fixed through photosynthesis is retained in the above- and below-ground biomass during the growing season, some C will be exuded through the roots and enter the soil system. The cultivation of perennial grasses, such as switchgrass with a root:shoot ratio of 1.8-6.1, increases soil organic carbon in the top 30 cm of soil by approximately 0.1–1 Mg ha<sup>-1</sup> yr<sup>-1</sup>, as roots and rhizomes are the primary method for C movement from biofuel crops to soil (Anderson-Teixeira et al., 2009). Furthermore, soluble root exudates and non-lignified root litter are easily metabolized by microorganisms in the rhizosphere, which emit CO<sub>2</sub> from respiration when abundant oxygen is present. When respiration is high and depletes the oxygen level in soil microsites, the redox conditions become suitable for other biochemical processes, such as N<sub>2</sub>O

production via denitrification and CH<sub>4</sub> production by methanogens (Brahmaprakash et al., 2017; Shah et al., 2020). Methanogens ferment acetate and use CO<sub>2</sub> as an electron acceptor for their metabolism process, which releases CH<sub>4</sub> as a by-product. Therefore, C cycling processes are connected with reactions in the N cycle and need to be considered simultaneously, supporting my decision to measure N<sub>2</sub>O, CO<sub>2</sub> and CH<sub>4</sub> in agricultural soil.

### **1.3 Factors contributing to the variation in CO<sub>2</sub> and N<sub>2</sub>O fluxes from soil-plant systems**

The CO<sub>2</sub> and N<sub>2</sub>O fluxes vary across agricultural fields because field soils are not homogeneous. Soil properties are fundamentally deterministic but soil parameters vary across spatial and temporal scales (Zou et al., 2018), creating an environment where aerobic and anaerobic microbial activities occur simultaneously. However, the pre-dominant aerobic or anaerobic activity in any spatio-temporal unit is related to the environmental conditions and available energy sources. Understanding the edaphic and environmental factors that influence the activities of soil microorganisms can give insight into the ‘hot spots’ and ‘hot moments’ of gas emissions. The edaphic factors that are influential for GHG fluxes are soil physical, chemical and biological properties, and the most important environmental factors are temperature and rainfall, which alter the soil temperature and soil moisture content (Yao et al., 2017). While physical properties like soil texture are relatively stable during longer periods of time (e.g., a growing season), we expect more spatio-temporal variability in soil chemical and biological properties (McDaniel et al., 2017). Short-term changes in soil chemistry, related to the concentration of soil organic carbon and nutrients, elicit responses in microbial activity, leading to the production of CO<sub>2</sub> and N<sub>2</sub>O gases. The heterogeneity of site-specific properties through space and time, which

control CO<sub>2</sub> and N<sub>2</sub>O fluxes in soil-plant systems, must be taken into consideration when selecting climate-smart management practices for agriculture.

### *1.3.1 Topography and soil type*

Topography influences GHG production because the distribution of water, organic matter, microbial populations and various other properties is less at higher slope positions than in lower slope positions across agricultural landscapes (Florinsky et al., 2004). The most important effect of topography, in determining the occurrence of aerobic vs. anaerobic microsites, is the way that topography influences precipitation flow patterns, water accumulation and erosion processes (Wiesmeier et al., 2019). Downslope positions have higher denitrifier enzyme activity than upslope positions and thus higher potential for denitrification (Florinsky et al., 2004). Field studies have found that relief accounted for 51% of the variation in denitrification potential (Li et al., 2018).

Soil types differ in their respiration and denitrification potential. Denitrification potential is highest in peat soils, followed by clay soil, loamy soils and sandy soils that have the lowest potential (Munch & Velthof, 2007). Peat soils have at least 60% organic matter, which can decompose and provide nutrients required for N<sub>2</sub>O emissions. Clay soils contain more micropores, which may provide more habitat for denitrifiers and support higher denitrification potential than loamy soils and sandy soils. Soil type and structure will give an indication of the porosity within the soil and thus the capacity of the soil to retain air, organic matter and water.

### *1.3.2 Soil temperature*

Soil temperature is positively correlated with increasing rates of GHG emissions. In a

subtropical climate study, temperature explained 26-59% of CO<sub>2</sub> flux variability across paddy, orchard, woodland and upland land-use types (Iqbal et al., 2008). A study of maize, soybean and maize-soybean intercropping systems demonstrated that log normalized N<sub>2</sub>O fluxes and temperature were positively associated, with a Pearson correlation coefficient of 0.207 ( $P < 0.05$ ) (Shen et al., 2018). The same study found a Pearson correlation coefficient of 0.614 ( $P < 0.01$ ) for CO<sub>2</sub> fluxes and temperature. Proximal soil sensing reveals that soil temperature and moisture are better predictors of the emission of CO<sub>2</sub> than N<sub>2</sub>O or CH<sub>4</sub> (McDaniel et al., 2017).

### *1.3.3 Soil moisture*

Moisture content is an important determinant of soil GHG emissions. Changes in moisture content influence the distribution of oxygen in the soil (Linn & Doran, 1984). Although N<sub>2</sub>O emissions occur in both aerobic and anaerobic conditions, a soil that experiences an increase in moisture content, as from after a rainfall event, can be expected to emit N<sub>2</sub>O at a higher rate. Fluxes of N<sub>2</sub>O from agricultural soils are highest after the application of the fertilizer and following heavy rainfall events (Monti et al., 2012). When sampling GHGs using soil surface gas chambers, it is considered good sampling practice to take chamber headspace measurements after soil rewetting events to capture the maximum GHG fluxes from the field.

### *1.3.4 Soil pH*

Soil pH is a limiting factor for the growth and activity of soil fauna and flora because it changes the efficacy of enzymatic reactions and the availability of nutrients that are metabolized and transformed in biogeochemical cycles (Hayatsu et al., 2008). Nitrogen-cycling

microorganisms may have a competitive advantage in a particular pH range. For instance, the ammonia oxidizer *Nitrosospira* is more abundant in acidic soils with pH 3 to 6. Denitrification is also influenced by the soil pH (Bouwman et al., 2002). Denitrification occurs at slower rates in acidic soils than in slightly alkaline soils. The product ratio of  $N_2O:N_2$  from denitrification is influenced by pH; at pH below 8,  $N_2O$  reductases are suppressed and the denitrification cycle is not completed, leading to the release of  $N_2O$  as the dominant product (Kunhikrishan et al., 2016). Furthermore, the reactive soil N concentration is lower in acidic soils (pH < 6.5) and in highly alkaline soils (pH > 7.5) than in soils with neutral pH conditions. When soil pH deviates from the optimal range of pH 6.5-7.5, the inhibition of extracellular proteases and urease involved in N mineralization reactions that produce  $NH_4^+$ , coupled with lower ammonia oxidation and nitrification rates, generate less reactive soil N (Kunhikrishan et al., 2016). Therefore, the highest  $N_2O$  fluxes from nitrification occur between pH 6 and 7, and denitrification-mediated  $N_2O$  fluxes are greater from pH 5-8.

#### **1.4 Conclusions and future directions**

In agricultural soils, naturally occurring biological processes like root and microbial respiration will produce  $CO_2$ , while microbial transformation of N substrates can generate  $N_2O$ . Applying more N fertilizer than required by crops increases the likelihood of  $N_2O$  emissions, but this depends upon soil conditions like moisture, temperature, pH, reactive soil N concentration and texture, which control the  $CO_2$  and  $N_2O$  fluxes. Developing an in-depth understanding of field variability and establishing a monitoring program to track the dynamic ancillary variables such as moisture and temperature can support the selection of climate-smart management practices that determine the ‘hot spots’ and ‘hot moments’ of  $CO_2$  and  $N_2O$  fluxes.

My thesis research involved the characterization of soil variability and delineation of homogenous soil zones to identify the variables that contribute to the hot spots and hot moments of CO<sub>2</sub> and N<sub>2</sub>O. The objectives of this study were to assess field variability, predict different zones in the field that could be susceptible to higher GHG fluxes and evaluate N fertilizer application rates on the production of N<sub>2</sub>O. I hypothesize that the hot spots will occur in the wetter areas of the field, 40-80% water-filled pore space, in the lower slope position and has slow-draining clay soils, where greater N<sub>2</sub>O will be produced than the drier hillslope with fast-draining sandy-loam soils. I hypothesize that the largest hot moment will occur following the first major rainfall event after the addition of N fertilizer, and other N<sub>2</sub>O peaks will be correlated with higher N rates, higher precipitation and higher soil temperatures. This study will expand on the understanding of field variability and the impacts of N fertilizer additions on GHG emissions. This study will help farmers and other agricultural decision makers to create recommendations for management practices that are site-specific and encompass an in-depth understanding of field variability and conditions.

## **Chapter 2: Management zone identification from soil properties and spectral images in a switchgrass field**

*Alexia M. Bertholon<sup>A,B</sup>, Joann K. Whalen<sup>A</sup>, Athyna Cambouris<sup>C</sup>, and Louis Longchamps<sup>D</sup>*

<sup>A</sup>Department of Natural Resource Sciences, McGill University, 21111 Lakeshore Road, Ste-Anne-de-Bellevue, QC, H9X 3V9, Canada.

<sup>B</sup>St-Jean-sur-Richelieu Research and Development Centre, Agriculture and Agri-Food Canada, 430 Gouin Boulevard, St-Jean-sur-Richelieu, QC, J3B 7B5, Canada.

<sup>C</sup>Québec Research and Development Centre, Agriculture and Agri-Food Canada, 2560 Hochelaga Boulevard, Québec, QC, G1V 2J3, Canada.

<sup>D</sup>Soil and Crop Sciences Section, School of Integrative Plant Science, Cornell University, Ithaca, NY, 14853, United States.

\*Corresponding author. Email: [louis.longchamps@cornell.edu](mailto:louis.longchamps@cornell.edu)

### **Summary text for the Table of Contents**

Commercial farms are looking for cost-effective ways to apply fertilizers needed by crops.

Because it is challenging to continually adjust the fertilizer applicator across non-uniform fields, the alternative is to set fertilizer rates for distinct management zones. Proximal sensors that measure apparent soil electrical conductivity and spectral reflectance were an effective alternative to traditional soil fertility testing for delineating the boundaries of fertilizer management zones in a perennial switchgrass system.

## **Abstract**

Soil fertility is generally uneven in agricultural fields, meaning that a uniform fertilizer application rate could be inadequate or provide excessive nutrients to the crop. Fertilizer applicators can be programmed to deliver variable fertilizer rates, but it is computationally demanding to adjust the fertilizer metering system continuously across heterogeneous fields. The objective of this study was to determine how many input variables are required to distinguish fertilizer management zones in a perennial switchgrass field (8.9 ha, located in southern Québec, Canada) based on (1) soil physicochemical properties in topsoil (0–20 cm) at 128 locations, (2) apparent electrical conductivity in the soil profile at 0.75 m and 1.5 m, and (3) a multispectral red, green and blue image of the bare (non-vegetated) soil surface. Apparent soil electrical conductivity was measured continuously at depths of 0.75 m and 1.5 m. Four field maps were drawn with Management Zone Analyst software, a geostatistical mapping program, and ArcGIS. Three management zones were identified in the reference map, which included soil physicochemical properties (C:N ratio, total sand, silt, clay, extractable phosphorous, total carbon, soil moisture, pH) along with coarse elevation and apparent soil electrical conductivity. Maps drawn from the electrical conductivity alone or with multispectral images also had three management zones. The definitive map of this field, with three management zones and 73% overlap in grouped areas relative to the reference map, used these parameters: electrical conductivity (0.75 m and 1.5 m), coarse elevation and the multispectral red, green and blue images of the bare soil surface.

**Keywords:** geostatistics, humid temperate agroecosystem, nitrogen fertilizer, proximal sensing, soil mapping, traditional soil fertility testing.

## 2.1 Introduction

Soil fertility varies across agricultural fields that have unequal topography, hydrology and soil-forming processes, resulting in a non-uniform crop yield. Since the 1990s, advances in remote sensing coupled with on-the-go yield monitoring have revealed soil fertility variation at the field scale (Pedersen & Lind 2017). Farmers need to describe the variability in soil fertility across fields, so they can adjust the fertilizer application rates according to the crop nutrient demands and expected yields. Computerized fertilizer application equipment such as the GreenStar™ Rate Controller, GreenStar™ 3 2630 and Rate Controller 2000 (Deere & Company, Moline, IL) provide control of the fertilizer application rate across the field. However, there are limits to the accuracy of this technology. For example, the GreenStar™ Rate Controller calculates the application rate from a smoothing function, which will apply fertilizer within 3-15 % of the rate specified by the operator (Deere & Company 2012). Therefore, there are limitations in the ability of variable rate fertilizer applicators to match the nutrient inputs with crop nutrient requirements across farm fields.

Since it is impossible to change the fertilizer application rate for every square meter of the farm field, the practical approach is to segregate the field into areas with similar soil fertility, known as management zones, and apply a targeted fertilizer rate to each zone. Management zones are assumed to have homogenous soil fertility and thus can be treated uniformly with respect to fertilizer application. Depending on the delineation method, management zones can be selected by calculating and assigning zone values for each data point provided by the user, which generates homogenous polygons that group the points according to their zone value. Typically, fields are divided into 2 to 4 management zones (Martínez-Casasnovas et al. 2018; Rossi et al. 2018; Moral & Serrano 2019). In a study on maize production in Colorado (USA), the field was

partitioned into 3 management zones drawn with Management Zone Analyst software (Cordero et al. 2019). Maize grain yield, N use efficiency and the farmer's net return were compared in each zone that received a targeted N fertilizer rate or the zone-specific, variable N fertilizer rate. The uniform N fertilizer rate was suitable in homogenous areas of the field, but the variable N fertilizer rate was a better predictor of yield and profitability in areas with greater spatial variability because the partial factor productivity could be improved by optimizing the grain yield relative to total amount of N supplied (based on crop proximal sensing in areas with <16 m spatial range or zone identification with Management Zone Analyst in areas with >100 m spatial range; Cordero et al. 2019).

Soil fertility parameters are often used to delineate management zones. This involves testing soil from discrete locations or by proximal soil sensing methods, which reflect soil conditions across the field area. Since boundaries are drawn across the field, discrete data like soil extractable nutrient concentrations, texture and pH must be transformed into continuous data using geostatistical analysis (Chilès & Delfiner 2012). Soil properties can also be estimated continuously with ground conductivity meters that rely on electromagnetic induction to monitor the apparent soil electrical conductivity. The apparent soil electrical conductivity is correlated with the clay content, volumetric water content and temperature (Baas et al. 2014). Although ground conductivity meters do not measure soil fertility directly, the apparent soil electrical conductivity is correlated with soil fertility indicators such as soil organic matter and cation exchange capacity (Moral & Serrano 2019). Furthermore, apparent soil electrical conductivity is correlated with crop yield. In a 27 ha field of wheat with 3 management zones, the highest mean crop yield of 4.80 t ha<sup>-1</sup> was in the management zone with a mean electrical conductivity of 0.74 dS m<sup>-1</sup> and the lowest mean crop yield of 2.22 t ha<sup>-1</sup> was in the management zone having a mean

electrical conductivity of 5.35 dS m<sup>-1</sup> (Yari et al. 2017). Apparent soil electrical conductivity is related to soil moisture and salinity, which inhibited growth in the low-yielding management zone due to water ponding and salt accumulation.

Multispectral satellite imagery, such as bare (non-vegetated) soil imagery, is another type of continuous data that describes field variability. Multispectral images capture the wavelengths of light that are reflected from a surface, i.e., the surface color. Soil moisture and organic matter concentration are the main determinants of the spectral properties of bare soils (Fleming et al. 2004). In an agricultural field, the bare soil color is an indication of water distribution in the field because wet or flooded soils have a darker color than dry soil (Vauclin et al. 1982; Ge et al. 2011; Georgi et al. 2018). Additionally, darker soils are associated with higher fertility and higher organic matter concentrations, and bare soil images gave a reliable prediction of soil C values ( $r^2=0.97$ ; Chen et al. 2000). Since bare soil images are associated with soil fertility parameters, they could be input data for management zone delineation.

The objective of this study was to determine how many input variables are required to distinguish management zones in a heterogeneous switchgrass field (8.9 ha) based on (1) soil physicochemical properties in topsoil (0–20 cm) at 128 locations, (2) apparent electrical conductivity measured continuously in the soil profile at 0.75 m and 1.5 m, and (3) a continuous multispectral red, green and blue image of the bare (non-vegetated) soil surface. The reference map in this study was the 10 Variables map developed by important soil properties defined in Longchamps and Khosla (2017), which considers the variability associated with soil physicochemical properties (C:N ratio, sand, silt, clay, extractable phosphorous, total carbon, moisture, pH) along with coarse elevation and apparent soil electrical conductivity (1.5 m). The similarity of boundaries and management zones of all other maps, drawn with fewer input

parameters, were compared with the reference map. We predicted that the proximal sensing data will provide enough information for management zone delineation, thereby reducing the need for time-consuming and costly soil testing.

## **2.2 Materials and methods**

### *2.2.1 Site description*

The experimental field is on a predominantly clay loam soil in the Cookshire-Eaton region (45°34' N, 71°78' W) approximately 10 km southeast of Sherbrooke, Québec Canada. Field soil is classified as a Podzol (Soil Classification Working Group 1998). The site receives approximately 1000 mm of precipitation annually with about 700 mm of precipitation from April to October (Environment Canada 2017). Switchgrass (*Panicum virgatum* L. cv Cave-in-Rock) was established in 2008, cultivated continuously and harvested once a year.

### *2.2.2 Soil sampling and physicochemical analysis*

Soil (0-20 cm) was sampled with a soil probe (4 cm diameter) on 25 May 2017 from 128 geo-referenced locations, recorded using an Arrow 200 GNSS Receiver with real time kinetic precision (Eos Positioning Systems, Terrebonne, Québec). Sampling locations were pre-determined with a stratified random sampling design (Dutilleul 2011), illustrated in Fig. 2-1. Samples were air-dried and sieved (<2 mm) before analysis. Soil pH was determined in 1:1 soil:deionized water slurries. Total carbon, total nitrogen and the C:N ratio were measured with a vario MACRO cube analyzer (Elementar, Langenselbold, Germany). Extractable nutrients (P, K, Ca, Mg, Al, Fe, Cu, Zn and Mn) in Mehlich III solution (1:10 soil:extractant) were analyzed with

the Optima 4300™ DV ICP-OES an ICP analyzer (PerkinElmer Inc., Waltham, MA). Soil physicochemical parameters are described in Table 2-1.



**Figure 2-1.** Soil sampling locations in an 8.9 ha switchgrass field in southern Québec, Canada.

The sampling pattern was a random within grid sampling design. The map was drawn in ArcMap (version 10.4.1) and the bare soil image was taken from Google Earth Pro (version 7.3.2.5776).

**Table 2-1.** Soil physicochemical properties (0–20 cm) in an 8.9 ha switchgrass field in southern Québec, Canada. Data are from 128 soil samples collected in May 2017.

<b>Physicochemical Property</b>	<b>Unit</b>	<b>Min<sup>A</sup></b>	<b>Max<sup>B</sup></b>	<b>Mean</b>	<b>SD<sup>C</sup></b>	<b>CV<sup>D</sup></b>
pH	(1:1)	5.71	6.94	6.25	0.26	4.2
Clay	g kg <sup>-1</sup>	46.4	133	74.8	15.2	20
Sand	g kg <sup>-1</sup>	237	712	425	113	27
Silt	g kg <sup>-1</sup>	181	712	500	124	25
Total Carbon (C)	g kg <sup>-1</sup>	16.3	63.3	30.4	8.05	27
Total Nitrogen (N)	g kg <sup>-1</sup>	1.19	4.42	2.23	0.549	25
Phosphorus (P)	mg kg <sup>-1</sup>	8.21	131	40.1	23.7	59
Potassium (K)	mg kg <sup>-1</sup>	32.8	227	72.3	27.7	38
Magnesium (Mg)	mg kg <sup>-1</sup>	24.4	147	69.9	22.9	33
Iron (Fe)	mg kg <sup>-1</sup>	129	642	352	117	33
Copper (Cu)	mg kg <sup>-1</sup>	2.07	11.8	3.90	1.31	34
Zinc (Zn)	mg kg <sup>-1</sup>	2.18	8.77	4.73	1.54	33
Manganese (Mn)	mg kg <sup>-1</sup>	11.3	293	74.9	59.7	80

<sup>A</sup>Min: Minimum. <sup>B</sup>Max: Maximum. <sup>C</sup>SD: Standard Deviation. <sup>D</sup>CV: Coefficient of Variation (%)

### *2.2.3 Apparent soil electrical conductivity and multispectral measurements*

Apparent soil electrical conductivity and coarse elevation were determined by proximal scanning with an EM38-MK2 (Geonics Limited, Mississauga, ON, Canada) to depths of 0.75 m and 1.5 m in the soil profile. The ground conductivity meter was pulled across the field along sequential east-west transects, starting at the northwest corner of the field and ending at the southeast corner of the field. The average distance between sampling scans was 9.74 m.

A red, green and blue image of the bare soil surface was extracted from Google Earth Pro (version 7.3.2.5776, Google, Mountain View, CA) using the “Historical imagery tool” to identify an image showing bare soil and the “Save image tool” to download the image in high definition (i.e., 1920 x 1080 pixels). Geo-rectification in ArcMap 10.4.1 (ESRI, Redlands, CA) matched the multispectral image to the georeferenced field boundaries. The image that was transferred into ArcMap contained the multispectral red, green and blue values, which were used as continuous input data in Management Zone Analyst.

### *2.2.4 Geostatistical analysis of soil physicochemical properties*

Spatial distribution of geolocated soil physicochemical parameters was described with a geostatistical method, following the procedure of Longchamps et al. (2015) in which autocorrelation among soil properties was evaluated with Moran’s I statistic, partial Moran’s I and P-values (Moran 1948). Soil properties that were autocorrelated ( $P < 0.05$ ) were used for data interpolation by semi-variogram analysis and kriging. The spherical, exponential and Gaussian semi-variogram models were tested to determine the best-fit semi-variogram model for each soil characteristic with R statistical software (version i386 3.4.1, Comprehensive R Archive Network, Vienna, Austria). The semi-variogram model with the lowest Akaike information

criterion value was considered the best-fit model (Webster & McBratney 1989), which was different for each autocorrelated soil physicochemical property in this study. Kriging following the procedure of Tripathi et al. (2017) produced a continuous estimate of each soil physicochemical property in unsampled areas of the field. The accuracy of predicted and actual measurements of each soil characteristic was cross-validated according to Longchamps et al. (2015).

Next, the interpolated map layers (i.e., one layer for each soil characteristic) were generated and transferred into ArcMap (Fig. 2-2, Fig. 2-3). A composite layer, which is a meta-file with all field data, was derived using the Fishnet tool from ArcMap. This tool generated points at 10 m intervals that linked the value for each soil characteristic (from the interpolated kriging map of the field) into a common vector file, and point values were deduced with the Spatial Analyst tool in ArcMap. Management Zone Analyst allows the user to select properties from the composite layer, giving a choice about which of the soil physicochemical properties are included in a particular map.

#### *2.2.5 Management zone delineation*

Management zones were delineated with Management Zone Analyst (version 1.0, USDA ARS, <https://www.ars.usda.gov/research/software/>). Parameters that could describe the field heterogeneity were the continuous data from soil physicochemical maps (one map for each soil variable), the apparent soil electrical conductivity at two depths (0.75 m and 1.5 m), field elevation map and the multispectral image of the field. All maps were drawn using the software default parameters (Fridgen et al. 2004), described in Table 2-2.

Post classification analysis in Management Zone Analyst generates graphs that are used to select the appropriate number of zones for a field based on the normalized classification entropy and the fuzziness performance index. Normalized classification entropy measures the homogeneity of the zones while the fuzziness performance index measures the degree of separation between the zones, which ranges from 0 to 1. If the fuzziness performance index value is closer to 0, then the zones are very distinct (i.e., the properties in one zone have different values from the properties in the other zone). Ideally, we wanted  $\leq 3$  management zones with different variable N fertilizer rates so the farmer could set a reasonable number of target N fertilizer rates to be delivered with a conventional fertilizer applicator (calibrated manually).

Four maps were produced with Management Zone Analyst. The Reference map set zone boundaries with the ten parameters: the C:N ratio, sand, silt and clay content, extractable phosphorous concentration, total carbon concentration, soil moisture, pH, coarse elevation and apparent soil electrical conductivity (1.5 m). The second map drawn from the apparent soil electrical conductivity (ECa 0.75 m and ECa 1.5 m) and coarse elevation data was called the ECa based map. The third Simple map included coarse elevation, ECa 0.75 m, ECa 1.5 m and multispectral images of red, blue and green bands. The fourth Texture map was generated from the total sand, silt and clay content.

**Table 2-2.** Parameters used to delineate map boundaries with Management Zone Analyst software.

Parameter	Selected value	Notes
Measure of similarity	Mahalanobis distance	Covariance $\neq$ 0
Fuzziness exponent	1.30	Limited membership sharing
Maximum number of iterations	300	
Convergence criterion	0.0001	
Minimum number of delineated zones	2	
Maximum number of delineated zones	6	

### 2.2.6 Comparing alternative maps to the Reference map

The data points were grouped with a fuzzy *c*-means unsupervised clustering algorithm, which accounted for continuous data by allowing each data point to be partial members of any group and terminated when the convergence criterion was met. Every map drawn with Management Zone Analyst had 878 coordinates that were assigned a management zone value of 1, 2 or 3, based on the unsupervised clustering algorithm. Each alternative map (ECa based, Simple, Texture) was compared to the Reference map to determine (1) if they had the same number of management zones and (2) if the coordinates were classified in the same management zone. The classification of coordinates in the management zones was determined with the `countif()` function in Excel (Microsoft Corporation, Redmond, WA). The percentage of coordinates that matched in the Reference and alternative maps was expressed as the % similarity between the two maps.

## 2.3 Results

### 2.3.1 Spatial autocorrelation of soil physicochemical properties

The 8.9 ha agricultural field was spatially heterogeneous, based on the switchgrass yields of 5 to 11 t dry matter ha<sup>-1</sup> across the field (personal communication with the farmer), visual

appearance and the measured soil test and proximal sensing data in this study. Most soil physicochemical properties in the agricultural field were spatially auto-correlated (Moran I,  $P < 0.05$ ). The only soil parameter that was not autocorrelated was potassium (K), which had a concentration of 32.8 to 149 mg K kg<sup>-1</sup> in 127 samples and one outlier that contained 227 mg K kg<sup>-1</sup> (Table 2-1), so it was excluded from the spatial analysis. Autocorrelated soil variables were: ECa 0.75 m, ECa 1.5 m, clay, sand, silt, pH, total carbon, total nitrogen, phosphorous, calcium, aluminum, cadmium, copper, magnesium, zinc and manganese. Kriging of autocorrelated soil variables showed two distinct sections of the field along a north to south transect, and this was associated with a soil texture gradient (e.g., see the variation in total sand content, Figure 2-2). These visual observations provide insight into the variability, which occurs gradually across the field, not in discrete areas of the field.

There was less variability in soil fertility parameters than the soil texture. For example, soil pH varied from 5.7 to 6.9 (Fig. 2-3) with some scattered zones of low and high pH. The variation in pH in this field probably did not affect switchgrass growth, since switchgrass growth is optimal from pH 5.0-8.0 and this crop is relatively insensitive to changes in soil pH (Martel & Lalonde 2018; Wolf & Fiske 2009). The lack of variation in soil pH and most other soil fertility indicators justify excluding these soil physicochemical parameters from management zone maps.

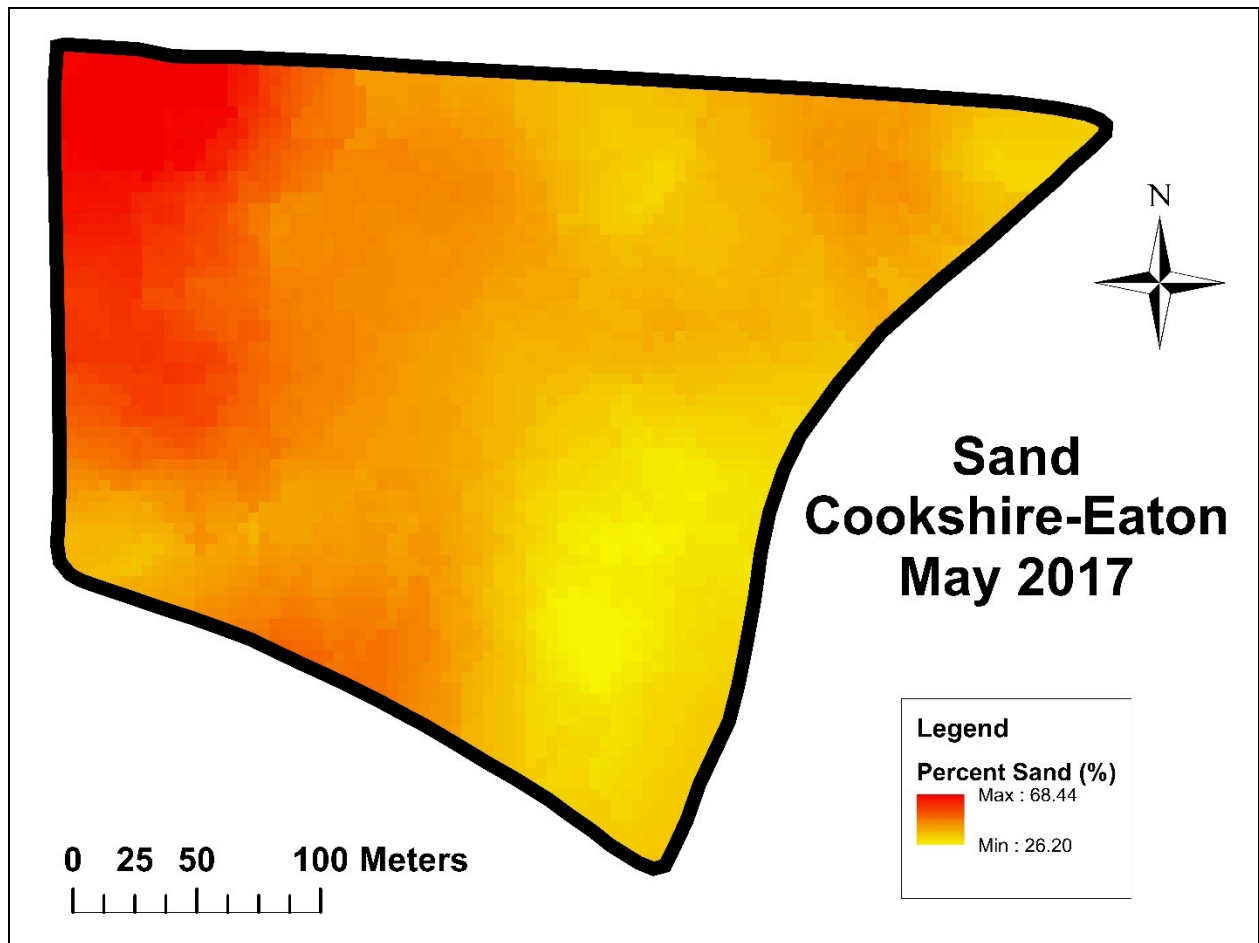


**Figure 2-2.** Total sand content, determined by geostatistical interpolation, in an 8.9 ha switchgrass field in southern Québec, Canada.

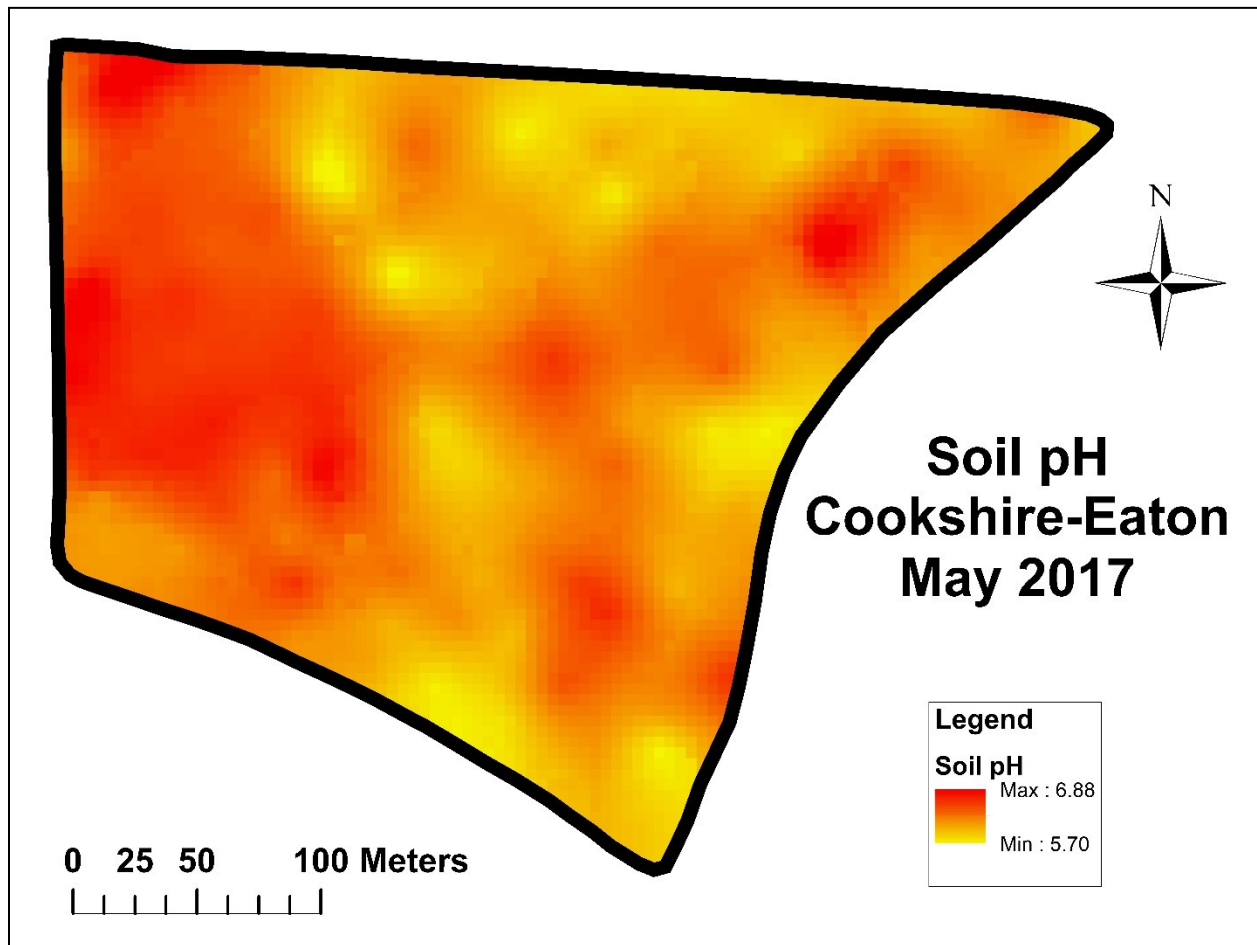


**Figure 2-3.** Soil pH determined by geostatistical interpolation, in an 8.9 ha switchgrass field in southern Québec, Canada.

### 2.3.2 Management zones

The Reference map and alternative maps had 3 management zones (Figs. 2-4, 2-5, 2-6 and 2-7). The Reference map was similar to the Simple map, since 73% of the coordinates were in the same management zone but differed from the ECa based map and the Texture map. When comparing the Reference and Simple maps, there was 79% similarity in the coordinates of Zone 1, 87% similarity in Zone 2 and 58% similarity in Zone 3 (Figs. 2-4 and 2-6). Descriptive

statistics of selected soil physicochemical properties in Zone 1 and Zone 3 of the Simple map are given in Table 2-3.

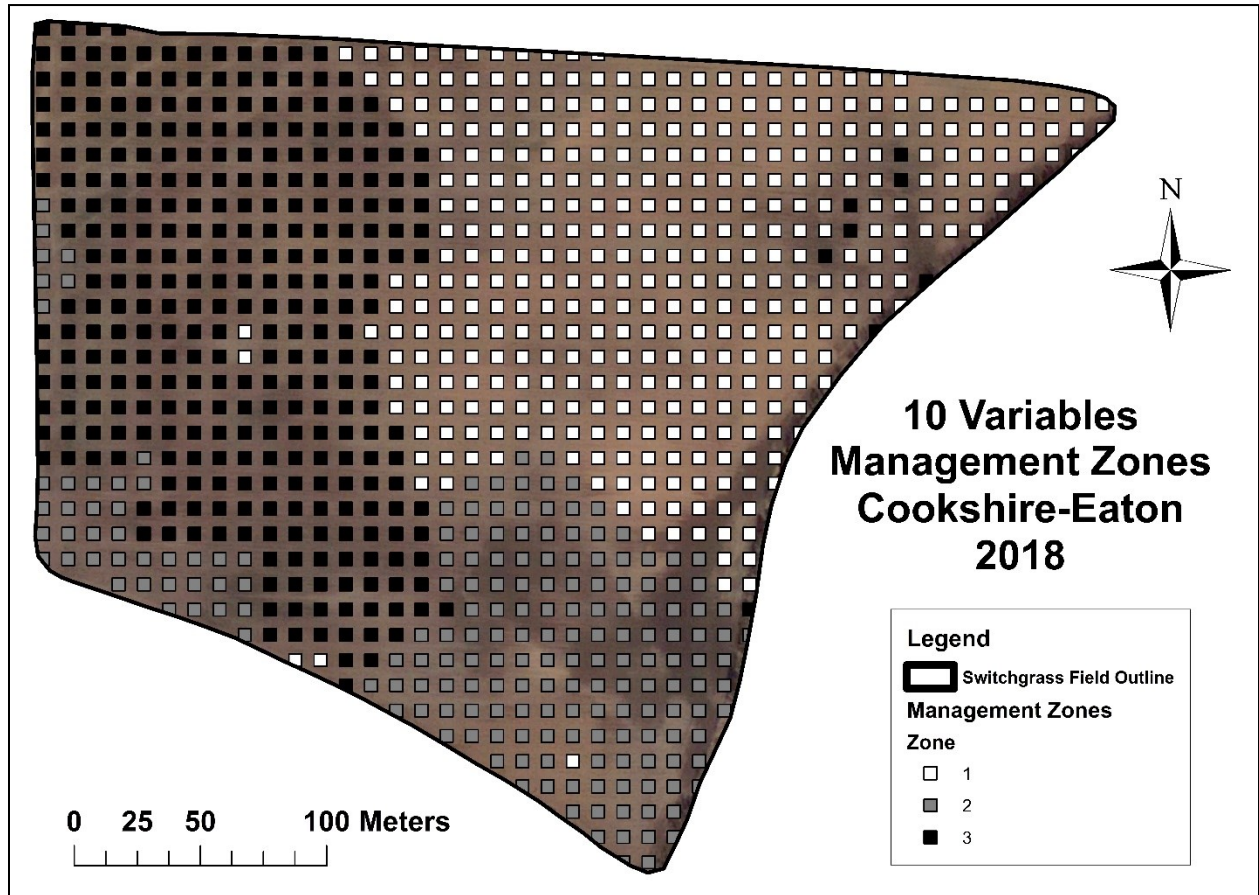


**Figure 2-4.** Reference map of an 8.9 ha switchgrass field in southern Québec, Canada. The map was drawn from 10 variables, including 8 soil physicochemical properties (C:N ratio, the total sand, silt and clay content, extractable phosphorous concentration, total carbon concentration, soil moisture content and pH) along with coarse elevation and apparent soil electrical conductivity (ECa 1.5 m), with Management Zone Analyst.

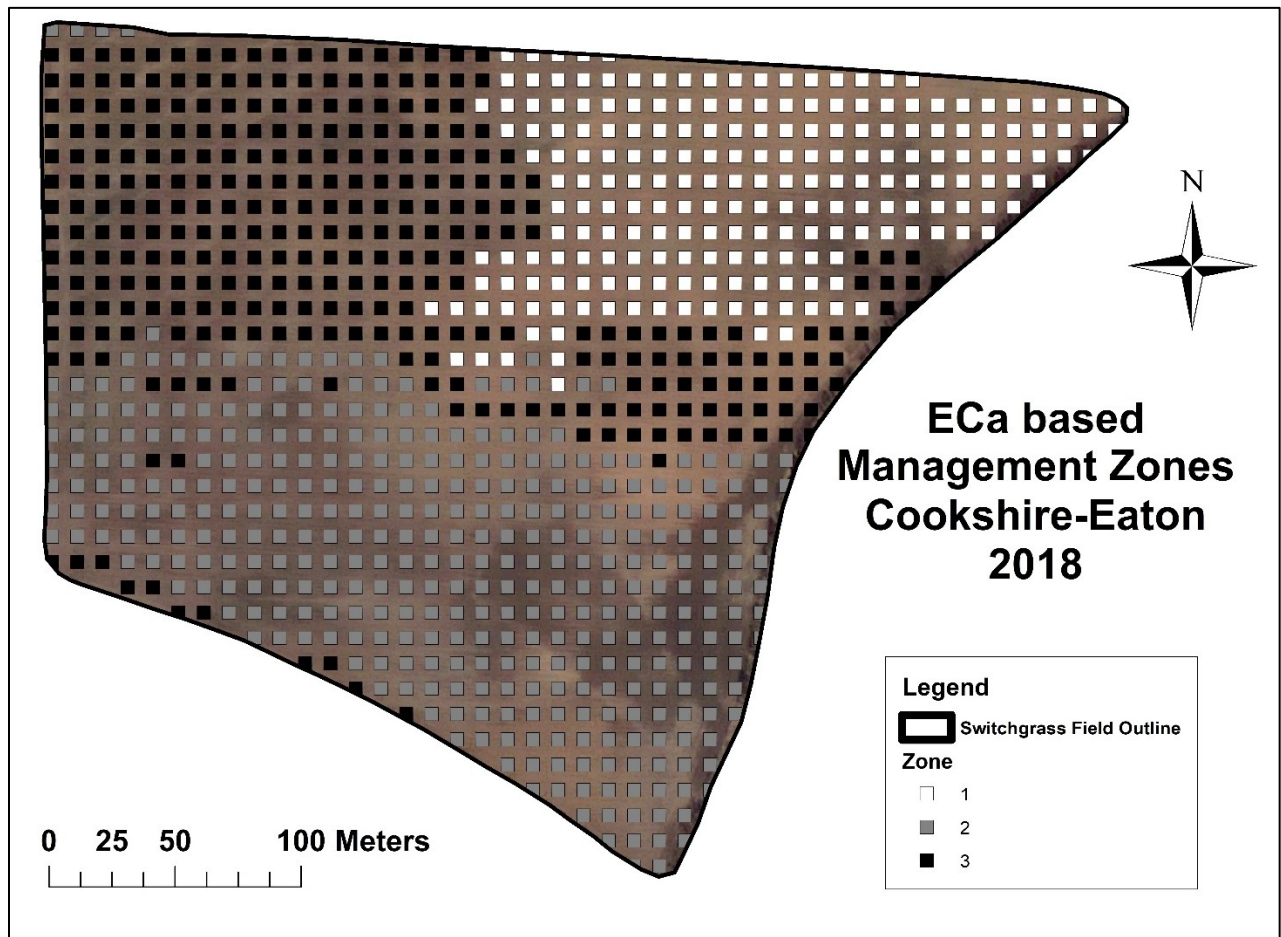


**Figure 2-5.** ECa based map of the 8.9 ha switchgrass field in southern Québec, Canada. The map was drawn from the coarse elevation and apparent soil electrical conductivity (ECa 1.5 m and ECa 0.75 m) data with Management Zone Analyst.

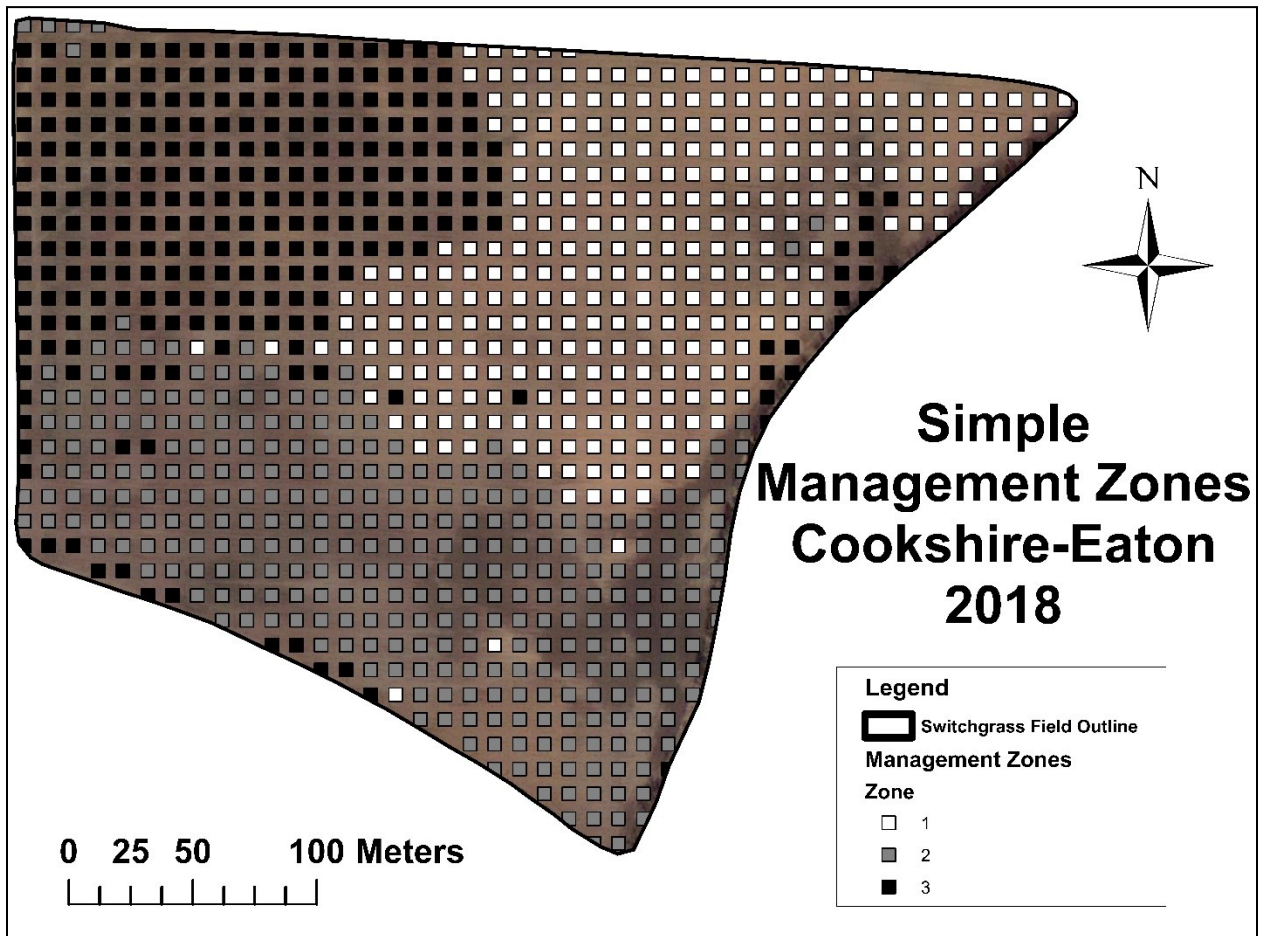


**Figure 2-6.** Simple map of the 8.9 ha switchgrass field in southern Québec, Canada. The map was drawn from the coarse elevation, apparent soil electrical conductivity (ECa 1.5 m and ECa 0.75 m) and the multispectral red, green and blue images of the bare soil surface with Management Zone Analyst.

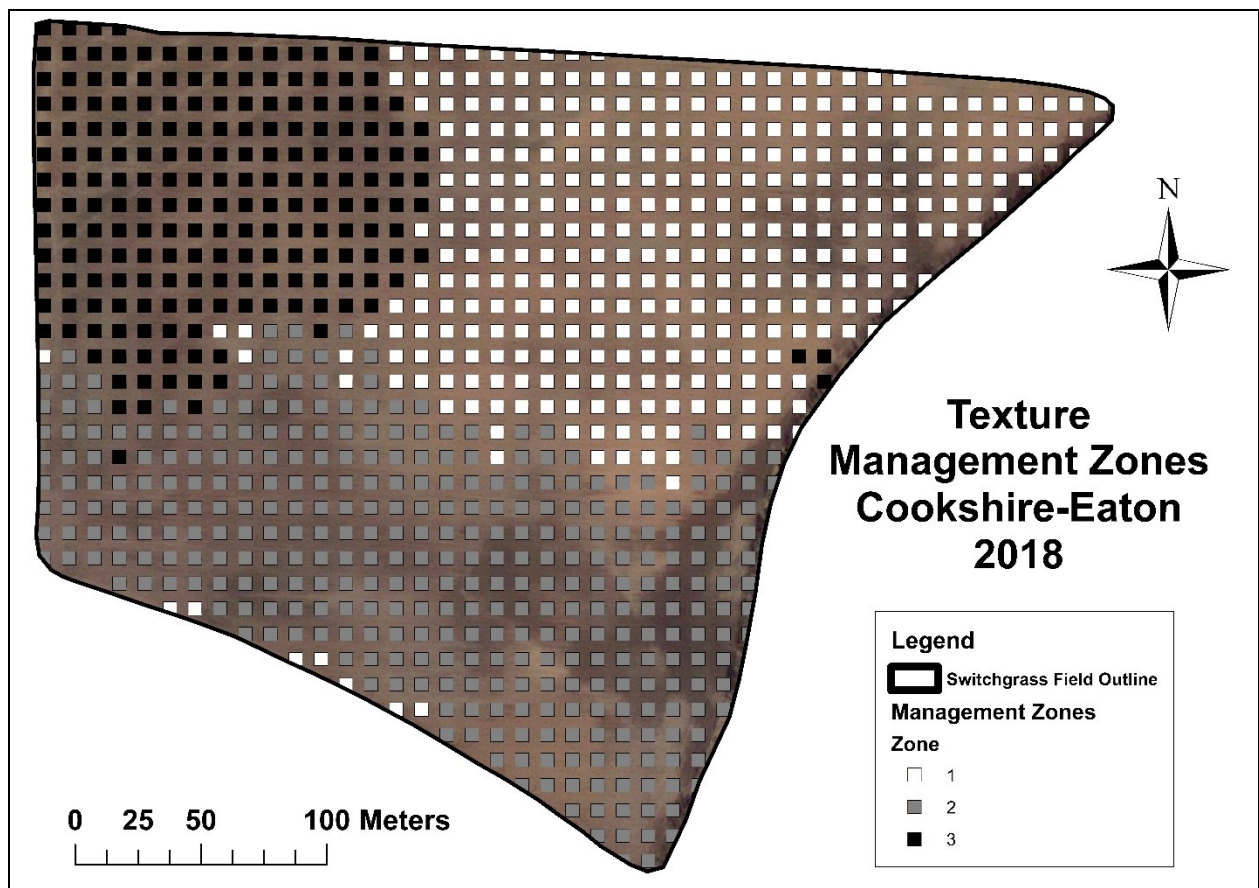


**Figure 2-7.** Texture map of the 8.9 ha switchgrass field in southern Québec, Canada, based on sand, silt and clay content, drawn with Management Zone Analyst.

**Table 2-3.** Descriptive statistics for selected physicochemical properties, apparent electrical conductivity and coarse elevation in Zones 1, 2 and 3 of the ‘Simple’ map of an 8.9 ha switchgrass field in southern Québec, Canada. The ‘Simple’ map is illustrated in Fig. 6.

Management Zone	Parameter	Unit	Min <sup>a</sup>	Max <sup>b</sup>	Mean	SD <sup>c</sup>	CV <sup>d</sup>
<b>Zone 1</b>	Sand	g kg <sup>-1</sup>	286	445	374	32.2	9
	Silt	g kg <sup>-1</sup>	464	664	554	38.6	7
	Clay	g kg <sup>-1</sup>	49.8	90.0	74.3	6.31	8
	Total carbon	g kg <sup>-1</sup>	23.9	38.9	32.9	2.37	7
	Mehlich-3 extractable P	mg kg <sup>-1</sup>	12.0	60.7	24.4	7.30	30
	pH	unitless	5.85	6.84	6.17	0.157	3
	ECa 0.75	mS m <sup>-1</sup>	41.4	46.6	43.6	0.92	2
	ECa 1.5	mS m <sup>-1</sup>	9.69	24.0	14.8	1.36	9
	Elevation	m	234	245	240	2.52	1
<b>Zone 2</b>	Sand	g kg <sup>-1</sup>	262	559	382	68.5	18
	Silt	g kg <sup>-1</sup>	334	703	550	80.3	15
	Clay	g kg <sup>-1</sup>	35.5	104	69.8	12.1	17
	Total carbon	g kg <sup>-1</sup>	23.4	54.2	32.4	5.74	18
	Mehlich-3 extractable P	mg kg <sup>-1</sup>	23.0	110	50.4	19.4	39
	pH	unitless	5.82	6.73	6.24	0.203	3
	ECa 0.75	mS m <sup>-1</sup>	42.7	50.8	46.4	1.17	3
	ECa 1.5	mS m <sup>-1</sup>	5.92	23.9	16.2	2.02	13
	Elevation	m	233	241	237	1.40	1
<b>Zone 3</b>	Sand	g kg <sup>-1</sup>	398	684	528	85.6	16
	Silt	g kg <sup>-1</sup>	210	530	393	101	26
	Clay	g kg <sup>-1</sup>	53.0	139	80.0	19.7	25
	Total carbon	g kg <sup>-1</sup>	18.0	34.4	24.7	2.87	12
	Mehlich-3 extractable P	mg kg <sup>-1</sup>	23.2	88.0	46.0	10.3	22
	pH	unitless	5.73	6.80	6.32	0.22	3
	ECa 0.75	mS m <sup>-1</sup>	42.4	49.2	45.3	1.19	3
	ECa 1.5	mS m <sup>-1</sup>	13.1	22.7	17.7	1.58	9
	Elevation	m	231	240	235	1.74	1

<sup>A</sup>Min: Minimum. <sup>B</sup>Max: Maximum. <sup>C</sup>SD: Standard Deviation. <sup>D</sup>CV: Coefficient of Variation (%)

## 2.4 Discussion

### 2.4.1 Site-specific management zone delineation

Our findings confirm that proximal soil sensing is appropriate to describe the spatial variability in this 8.9 ha switchgrass field. Like the Reference map, the maps derived from proximal sensing data, i.e., the Simple map and the ECa based map, identified three management

zones. As many producers continue to adjust their fertilizer applicator manually rather than with automated on-the-go metering systems, it is considered to be more practical to identify 2 to 4 management zones per field (Shukla et al. 2017; Rossi et al. 2018; Martínez-Casasnovas et al. 2018; Moral & Serrano 2019). Therefore, three management zones is a reasonable number for this field, based on the producer's goal of achieving a consistent, high switchgrass yield in this heterogeneous field with a reasonable investment of time and labor (i.e., to calibrate the fertilizer equipment and apply the target fertilizer rate to each zone) for this commercial farm operation.

Proximal soil sensing data gave a robust estimate of the management zone boundaries in this field. While the Reference map relied on soil physicochemical parameters, most of which were derived from traditional soil sampling and testing methods, the ECa based map was drawn from proximal soil sensing data and the Simple map combined proximal soil sensing and spectral reflectance data. The definitive feature of the Simple map was the inclusion of multispectral red, green and blue images of the soil surface, along with topographical (coarse elevation) and hydrological (apparent soil electrical conductivity) features. Spectral reflectance at the soil surface is strongly correlated with soil carbon and nitrogen levels, and to a lesser extent with the soil textural properties in the surface layer (Ahmadi et al. 2021). Furthermore, color images of the soil surface taken with the digital camera of a cell phone camera are associated with the soil organic matter level and soil moisture content (Taneja et al. 2021). This suggests that the multispectral images included in the Simple map were useful for the proxy measurement of soil physicochemical properties like the C:N ratio, total carbon, sand, silt and clay content, as well as the soil moisture content, which were included explicitly in the Reference map.

Zones 1 and 2 showed good correspondence ( $\pm 21\%$  difference) between the Reference map and the Simple map. Fluctuations in the total carbon level and sand content were major

sources of variation in these zones, and these characteristics were described by direct measurement of total carbon and sand in the Reference map and by proxy with the spectral reflectance data in the Simple map. However, there was 42% difference in group classification of the coordinates of Zone 3 in the Reference and Simple maps. Zone 3 had a higher sand content and less total carbon compared to the other zones, which could affect the interpretation of spectral reflectance data that is strongly correlated with soil carbon and soil organic matter measurements (Ahmadi et al. 2021; Taneja et al. 2021). This observation is further evidence that spectral reflectance data in the Simple map described heterogeneous features related to soil carbon, but whether spectral reflectance was more strongly associated with the total carbon or soil organic matter level at this site remains to be determined, since soil organic matter was not measured in this study. We conclude that spectral reflectance data can describe the spatial variation in soil fertility of zones with 23 to 54 g total carbon kg<sup>-1</sup> but may not fully represent the inherent soil heterogeneity in zones with lower total carbon content.

#### *2.4.2 Management Zone Analyst, a practical tool to make maps from proximal soil sensing data*

Proximal soil sensing is a way to describe soil spatial variability because it is associated with soil physicochemical parameters and other site-specific factors that are responsible for the heterogeneity in farm fields. Shaner et al. (2008) argued that ECa is the most important variable, other than historical yield, needed to delineate management zones. We agree with this statement because we found greater overlap of the Reference map with the Simple and ECa based maps, both of which included ECa measurements, than the Texture map, which did not. However, we acknowledge that ECa 1.5 m was included in the Reference map, meaning that it was already adjusted for the underlying hydrologic processes in these fields. Still, it was relatively simple and

cost-effective to collect the proximal soil sensing data for this study. For example, collection and processing of ECa and multispectral imagery data takes no more than 2 wk. One pass of the EM38-MK2 meter provided information on hundreds of points of elevation and ECa continuously across a field, and the data can be used as direct input to the spatial mapping software. This differs from soil physicochemical parameters, which must be taken from discrete locations and analyzed in a certified laboratory.

After the continuous spatial soil input data is collected or generated, it can be analyzed by Management Zone Analyst. Users can compare spatial statistics and ranges of grouping recommendations to determine the number of management zones that represent the field variability for practical agronomic actions. Once data was collected and processed, it took < 7 d to compare the zone delineation options using Management Zone Analyst. Management Zone Analyst could be improved by linking to a library with soil fertility groups for a particular geographical location, allowing the user to classify zones as low, medium or high fertility, to suggest lime application rates or organic amendments that could be helpful, and potentially to identify zones that are at a greater risk of emitting greenhouse gases, soil erosion and nutrient losses. Another possibility would be to add algorithms to generate and compare maps from field-based and proximal soil sensing, to reveal the root causes of soil heterogeneity in fields.

Proximal soil sensing with ECa and multispectral imagery can set appropriate boundaries for management zones, but more research is required to support the wide use of these methods as maps generated from these indirect measurement techniques are based on correlations rather than direct information about soil properties. It will be important to continue discrete soil sampling and testing in parallel with proximal soil sensing to produce more robust estimates of soil spatial variation across many soil types and agro-climatic conditions (Mendes et al. 2019). We

recommend continued study of ECa and multispectral imagery to validate the relationships between these proximal data and soil physicochemical properties, for better future predictions of soil fertility and productivity across heterogeneous farm fields.

## **2.5 Conclusion**

Farmers who wish to deploy variable-rate fertilizer technology in their fields are often discouraged by the fact that traditional soil mapping can be a time-consuming and expensive process that requires the collection and analysis of hundreds or thousands of soil samples to identify soil fertility gradients. This study demonstrated that proximal soil sensing data could provide robust information to set the boundaries of management zones. The proximal data from ECa, coarse elevation and multispectral imagery produced a Simple map that was comparable to the Reference map, with 58 to 87% correspondence in the area of three management zones between the maps. Multispectral images of the soil surface may represent the total carbon level, which was as much as 3 times lower in the sandier zone of the switchgrass field under study. While such proximal soil sensing datasets hold promise for partitioning management zones, the spectral reflectance measurement seems to be sensitive to the soil carbon or soil organic matter level, although this needs to be verified in other locations and production systems. We recommend that agricultural practitioners integrate proximal soil sensing in their spatial maps, since these measurements are relatively inexpensive and easy to incorporate into management zone analysis.

## **Data Availability**

The datasets generated during and/or analysed during the current study are available from the corresponding author on reasonable request.

## **Conflicts of Interest**

The authors declare no conflicts of interest.

## **Acknowledgements**

Funding for this project came from Agriculture & Agri-Food Canada. Alexia Bertholon would like to thank McGill University for the financial support provided by the Graduate Excellence Fellowship, Centre SÈVE and the Soil Ecology Research Group for travel award funding. The authors thank the staff of Agriculture & Agri-Food Canada at the Sainte-Foy and Saint-Jean-sur-Richelieu research centers for technical assistance and the cooperating producer for access to the field site.

## References

- Ahmadi, A., Emami, M., Daccache, A., & He, L. Y. (2021). Soil properties prediction for precision agriculture using visible and near-infrared spectroscopy: A systematic review and meta-analysis. *Agronomy-Basel*, *11*(3), 433.  
<https://doi.org/10.3390/agronomy11030433>
- Baas, P., Mohan, J. E., Markewitz, D., & Knoepp, J. D. (2014). Assessing heterogeneity in soil nitrogen cycling: A plot-scale approach. *Soil Science Society of America Journal*, *78*, S237–S247. <https://doi.org/10.2136/sssaj2013.09.0380nafsc>
- Chen, F., Kissel, D. E., West, L. T., & Adkins, W. (2000). Field-scale mapping of surface soil organic carbon using remotely sensed imagery. *Soil Science Society of America Journal*, *64*(2), 746–753. <https://doi.org/10.2136/sssaj2000.642746x>
- Chilès, J.-P., & Delfiner, P. (2012). *Geostatistics: Modeling spatial uncertainty*, 2<sup>nd</sup> edn. John Wiley & Sons, Inc. <https://doi.org/10.1002/9781118136188>
- Cordero, E., Longchamps, L., Khosla, R., & Sacco, D. (2019). Spatial management strategies for nitrogen in maize production based on soil and crop data. *Science of the Total Environment*, *697*, 133854. <https://doi.org/10.1016/j.scitotenv.2019.133854>
- Deere & Company. (2012). *GreenStar Rate Controller. Operator's Manual, OMPFP12328, Issue E2*. Deere & Company.  
[https://stellarsupport.deere.com/site\\_media/pdf/en/manuals/rate\\_controller/omfpf12328\\_RateController\\_EN.pdf](https://stellarsupport.deere.com/site_media/pdf/en/manuals/rate_controller/omfpf12328_RateController_EN.pdf)
- Dutilleul, P. (2011). *Spatio-temporal heterogeneity: Concepts and analyses*. Cambridge University Press.

- Environment Canada. (2017). *Monthly meteorological summaries for Sherbrooke*. Atmospheric Environment Branch, Environment Canada. <https://climate.weather.gc.ca/>
- Fleming, K. L., Heermann, D. F., & Westfall, D. G. (2004). Evaluating soil color with farmer input and apparent soil electrical conductivity for management zone delineation. *Agronomy Journal*, *96*(6), 1581–1587. <https://doi.org/10.2134/agronj2004.1581>
- Fridgen, J. J., Kitchen, N. R., Sudduth, K. A., Drummond, S. T., Wiebold, W. J., & Fraisse, C. W. (2004). Management Zone Analyst (MZA): Software for subfield management zone delineation. *Agronomy Journal*, *96*(1), 100–108. <https://doi.org/10.2134/agronj2004.0100>
- Ge, Y. F., Thomasson, J. A., & Sui, R. X. (2011). Wireless-and-GPS system for cotton fiber-quality mapping. *Precision Agriculture*, *13*(1), 90–103. <https://doi.org/10.1007/s11119-011-9225-6>
- Georgi, C., Spengler, D., Itzerott, S., & Kleinschmit, B. (2018). Automatic delineation algorithm for site-specific management zones based on satellite remote sensing data. *Precision Agriculture*, *19*(4), 684–707. <https://doi.org/10.1007/s11119-017-9549-y>
- Longchamps, L., Khosla, R., Reich, R., & Gui, D. W. (2015). Spatial and temporal variability of soil water content in leveled fields. *Soil Science Society of America Journal*, *79*(5), 1446–1454. <https://doi.org/10.2136/sssaj2015.03.0098>
- Longchamps, L., & Khosla, R. (2017). Precision maize cultivation techniques. In D. Watson (Ed.), *Achieving sustainable cultivation of maize: Cultivation techniques, pest and disease control* (pp. 107–148). Burleigh Dodds Science Publishing. <https://doi.org/10.19103/AS.2016.0002.07>

- Martel, H., & Lalonde, O. (2018). *Panic érigé: guide de production*. Réseau des plantes bio-industrielles du Québec. <https://www.agrireseau.net/documents/96746/panic-erige-guide-de-production>
- Martínez-Casasnovas, J. A., Escolà, A., & Arnó, J. (2018). Use of farmer knowledge in the delineation of potential management zones in precision agriculture: A case study in maize (*Zea mays* L.). *Agriculture-Basel*, 8(6), Article 84. <https://doi.org/10.3390/agriculture8060084>
- Mendes, W. d. S., Medeiros Neto, L. G., Demattê, J. A. M., Gallo, B. C., Rizzo, R., Safanelli, J. L., & Fongaro, C. T. (2019). Is it possible to map subsurface soil attributes by satellite spectral transfer models? *Geoderma*, 343, 269-279. <https://doi.org/10.1016/j.geoderma.2019.01.025>
- Moral, F. J., & Serrano, J. M. (2019). Using low-cost geophysical survey to map soil properties and delineate management zones on grazed permanent pastures. *Precision Agriculture*, 20, 1000–1014. <https://doi.org/10.1007/s11119-018-09631-9>
- Moran, P. A. P. (1948). The interpretation of statistical maps. *Journal of the Royal Statistical Society Series B – Statistical Methodology*, 10(2), 243–251.
- Pedersen, S. M., & Lind, K. M., (2017). Precision Agriculture – From mapping to site-specific application. In S.M. Pedersen & K. M. Lind (Eds.), *Precision agriculture: technology and economic perspectives* (pp. 1-20). Springer International Publishing. <https://doi.org/10.1007/978-3-319-68715-5>
- Rossi, R., Pollice, A., Bitella, G., Labella, R., Bochicchio, R., & Amato, M. (2018). Modelling the non-linear relationship between soil resistivity and alfalfa NDVI: a basis for

- management zone delineation. *Journal of Applied Geophysics*, 159, 146–156.  
<https://doi.org/10.1016/j.jappgeo.2018.08.008>
- Shaner, D. L., Khosla, R., Brodahl, M. K., Buchleiter, G. W., & Farahani, H. J. (2008). How well does zone sampling based on soil electrical conductivity maps represent soil variability? *Agronomy Journal*, 100(5), 1472-1480. <https://doi.org/10.2134/agronj2008.0060>
- Shukla, A. K., Sinha, N. K., Tiwari, P. K., Prakash, C., Behera, S. K., Lenka, N. K., Singh, V. K., Dwivedi, B. S., Majumdar, K., Kumar, A., Srivastava, P. C., Pachauri, S. P., Meena, M. C., Lakaria, B. L., & Siddiqui, S. (2017). Spatial distribution and management zones for sulphur and micronutrients in Shiwalik Himalayan region of India. *Land Degradation & Development*, 28(3), 959–969. <https://doi.org/10.1002/ldr.2673>
- Soil Classification Working Group (1998). *The Canadian system of soil classification*, 3rd ed. Agriculture and Agri-Food Canada. <https://sis.agr.gc.ca/cansis/taxa/cssc3/index.html>
- Taneja, P., Vasava, H. K., Daggupati, P., & Biswas, A. (2021). Multi-algorithm comparison to predict soil organic matter and soil moisture content from cell phone images. *Geoderma*, 385, 114863. <https://doi.org/10.1016/j.geoderma.2020.114863>
- Tripathi, R., Nayak, A. K., Raja, R., Shahid, M., Mohanty, S., Lal, B., Gautam, P., Panda, B. B., Kumar, A., & Sahoo, R. N. (2017). Site-specific nitrogen management in rice using remote sensing and geostatistics. *Communications in Soil Science and Plant Analysis*, 48(10), 1154–1166. <https://doi.org/10.1080/00103624.2017.1341907>
- Vauclin, M., Vieira, S. R., Bernard, R., & Hatfield, J. L. (1982). Spatial variability of surface-temperature along 2 transects of a bare soil. *Water Resources Research*, 18(6), 1677–1686. <https://doi.org/10.1029/WR018i006p01677>
- Webster, R., & McBratney, A. B. (1989). On the Akaike Information Criterion for choosing

models for variograms of soil properties. *Journal of Soil Science*, 40(3), 493-496.

<https://doi.org/10.1111/j.1365-2389.1989.tb01291.x>

Wolf, D. D., & Fiske, D. A. (2009). *Planting and managing switchgrass for forage, wildlife, and conservation*. Virginia Cooperative Extension.

<https://vtechworks.lib.vt.edu/bitstream/handle/10919/50258/418-013.pdf>

Yari, A., Madramootoo, C. A., Woods, S. A., Adamchuk, V., & Huang, H.-H. (2017).

Assessment of field spatial and temporal variabilities to delineate site-specific management zones for variable-rate irrigation. *Journal of Irrigation and Drainage*

*Engineering*, 143(9), 04017037. [https://doi.org/10.1061/\(ASCE\)IR.1943-4774.0001222](https://doi.org/10.1061/(ASCE)IR.1943-4774.0001222)

### **Connecting Paragraph**

In Chapter 2, I established that the agricultural field selected for my study was heterogeneous in its soil physicochemical properties, apparent soil electrical conductivity and spectral images. I delineated three management zones for the field, based on their elevation, soil hydrology (derived from the apparent soil electrical conductivity) and color (determined from the multispectral red, green and blue images of the bare soil surface). In Chapter 3, I will use my definitive field map to design a field experiment with replicated N fertilizer treatments in each management zone. The purpose of this experiment is to evaluate the effect of N fertilizer rates on N<sub>2</sub>O emissions and switchgrass yield.

### **Chapter 3: Variable rate nitrogen fertilizer application induces hot moments in nitrous oxide emissions in a switchgrass field in Southern Québec, Canada**

*Alexia M. Bertholon<sup>A,B</sup>, Joann K. Whalen<sup>A</sup>, and Louis Longchamps<sup>C</sup>*

<sup>A</sup>Department of Natural Resource Sciences, McGill University, 21111 Lakeshore Road, Ste-Anne-de-Bellevue, QC, H9X 3V9, Canada.

<sup>B</sup>St-Jean-sur-Richelieu Research and Development Centre, Agriculture and Agri-Food Canada, 430 Gouin Boulevard, St-Jean-sur-Richelieu, QC, J3B 7B5, Canada.

<sup>C</sup>Soil and Crop Sciences Section, School of Integrative Plant Science, Cornell University, Ithaca, NY, 14853, United States.

\*Corresponding author. Email: alexia.bertholon@mail.mcgill.ca

## Abstract

Nitrogen (N) fertilizer is essential for crop production but is susceptible to reactions that produce nitrous oxide (N<sub>2</sub>O), a potent greenhouse gas. Matching the N fertilizer inputs to crop N requirements should reduce the amount of reactive N that is lost from the agroecosystem as N<sub>2</sub>O. It is difficult to predict where these reactions will produce ‘hot spots’ of high N<sub>2</sub>O fluxes in a field, as well as the ‘hot moments’ when peak N<sub>2</sub>O fluxes occur. The objective of this study was to determine if applying variable rates of N fertilizer to heterogeneous zones would reduce the N<sub>2</sub>O emissions from a *Panicum virgatum* L. (switchgrass) field. Four N fertilizer application rates of 0x, 1x, 2x and 3x were applied to blocks (15 m x 100 m) in the high-yielding switchgrass zone and the low-yielding switchgrass zone of the field. Then, the N<sub>2</sub>O fluxes were determined by sampling headspace from non-flow-through, non-steady-state chambers (n=3 per block) every 7-10 d during the growing season. The “hot moment” of peak N<sub>2</sub>O flux occurred within 30 d of N fertilizer application, after rainfall events. Although N<sub>2</sub>O fluxes differed in the management zones in 2018, there were no distinctive “hot spots” in the switchgrass field in the 2019 growing season. Cumulative N<sub>2</sub>O emission tended to increase when higher N fertilizer rates were applied, suggesting that applying more N fertilizer increased the risk of gaseous N loss, probably through denitrification. In conclusion, geospatial analysis of agricultural fields can identify soil zones that are susceptible to N<sub>2</sub>O fluxes, although the magnitude of those fluxes depends upon N fertilizer rates, climatic conditions and cropping systems.

## 3.1 Introduction

Agricultural crops are generally fertilized with mineral N fertilizer to achieve yield

targets, but the soluble  $\text{NH}_4^+$ ,  $\text{NO}_2^-$  and  $\text{NO}_3^-$  released from N fertilizer are susceptible to undergo biological reactions that produce  $\text{N}_2\text{O}$ . Since the  $\text{N}_2\text{O}$  emissions increase exponentially as the N fertilizer rate increases, according to a meta-analysis of 84 agricultural fields (Shcherbak et al., 2014), this means that  $\text{N}_2\text{O}$  losses are more likely when more N fertilizer is applied. Consequently, it is necessary to optimize the N fertilizer application to reduce the risk that reactive N from fertilizer will undergo  $\text{N}_2\text{O}$  producing reactions. Optimization of the N fertilizer application must be done on a site-specific basis to closely match the N fertilizer input with the crop N requirements, thereby avoiding an excess of reactive N that can be biologically transformed to  $\text{N}_2\text{O}$ .

Applying a variable rate of mineral N fertilizer is an effective way to control  $\text{N}_2\text{O}$  emissions and N use efficiency in agricultural field. For instance, in low yielding zones of a maize field, site-specific variable rate N fertilizer application zones applied with  $125 \text{ kg N ha}^{-1}$  reduced  $\text{N}_2\text{O}$  release by 34% with equal crop yields to control treatments applied with  $150 \text{ kg N ha}^{-1}$  (Sehy et al., 2003). The low yielding zones in Sehy et al. (2003) were on a rounded hilltop and the reduction in  $\text{N}_2\text{O}$  release from the lower fertilization rate likely resulted from  $\text{N}_2\text{O}$  being directly related to soil  $\text{NO}_3^-$  content as waterlogging, which increased  $\text{N}_2\text{O}$  release in high yielding footslope position of the field, was not an issue at the hilltop. Schwalbert et al. (2019) found that adjusting the N fertilizer rate in a heterogeneous agricultural field improved the N uptake ( $p < 0.05$ ) in high yielding management zones and had an interaction with the grain yield ( $p < 0.05$ ) of wheat in different management zones. In this study, variability in the field was characterized by apparent electrical conductivity (ECa), topographic features (elevation and slope) and plant attributes (wheat vegetation index and maize grain yield). The management zone effect on plant N uptake was found when the application rate was  $120$  and  $160 \text{ kg N ha}^{-1}$ , when

plant N is less reliant on soil mineralization. However, there was no increase in plant N uptake in low yielding management zones, regardless of fertilizer application rate. When a constant N fertilizer rate is applied, the soil-plant system may tend to have excessive N, which is susceptible to leaching, denitrification and volatilization. Since additional N fertilizer application does not always result in increased N uptake and grain yield, Schwalbert et al. (2019) advocate for variable rate N fertilizer application. They found that variable N fertilizer application can reduce N<sub>2</sub>O emissions across management zones with distinct soil hydrology. These studies suggest that variable rate N fertilizer application can potentially reduce N<sub>2</sub>O emissions in fields with variable topography and hydrologic conditions. Although this may be true in annual crop production systems, it still needs to be evaluated in perennial cropping systems such as those with permanent grass cover like the switchgrass field described in Chapter 2.

The objectives of this study were to (1) evaluate N<sub>2</sub>O fluxes in response to the application of variable rates of N fertilizer in two management zones within a switchgrass field, (2) describe spatial variation in N<sub>2</sub>O fluxes in relation to the inherent variability in soil physicochemical properties and crop growth, and (3) evaluate the temporal variation in N<sub>2</sub>O fluxes in relation to environmental variables (e.g., soil moisture, soil temperature, precipitation). I hypothesize that (1) the control of 0 kg N ha<sup>-1</sup> will have significantly lower N<sub>2</sub>O emissions than the other three fertilizer rates and (2) that the management zone with greater soluble N concentration (due to less plant growth and higher N fertilizer rates) will produce more N<sub>2</sub>O during periods when the field is temporarily waterlogged (i.e., after rainfall).

## 3.2 Materials and Methods

### 3.2.1 Site description

The experimental site was located in the Cookshire-Eaton region (45°34' N, 71°78' W) approximately 10 km southeast of Sherbrooke, Québec, Canada. The field soil is classified as a Podzol with a sandy-loam texture, based on the field average of 75 g clay kg<sup>-1</sup> and 425 g sand kg<sup>-1</sup>. The site receives about 1000 mm of precipitation annually with approximately 700 mm of precipitation occurring from April to October (Environment Canada, 2017). The field has been continuously cultivated with switchgrass (*Panicum virgatum* L. cv Cave-in-Rock) since 2008. The switchgrass is harvested once a year, in May.

### 3.2.2 Experimental design

The switchgrass field had 3 distinct management zones (Chapter 2), and zones 1 and 3 were chosen for this study. The area of Zone 1 and Zone 3 were both approximately 2.22 ha<sup>-1</sup>. Next, this area was divided into eight treatment strips, each approximately 100 m x 15 m. The treatments were N fertilizer rates, assigned at random to strips in 2018 and repeated in the same strips in the second growing season, 2019. The N fertilizer was granular urea (46-0-0) broadcast via a tri-disk centrifugal spreader across the strip at rates of 0, 16.5, 33, 49.5 kg N ha<sup>-1</sup> on 31 May 2018 and 0, 50, 100, 150 kg N ha<sup>-1</sup> on 18 June 2019.

### 3.2.3 Gas sampling and analysis

A grid design was used for gas sampling, with bases spread out in an equal grid distance

15 m apart from one another. Bases were installed directly, within 1 h after fertilizer was applied to zone 1 and zone 3, in both sampling years. A total of 24 bases, with 12 bases per zone and  $n=3$  per strip, were installed in the field using a GPS (Arrow Series GNSS Receiver, EOS Positioning Systems, Terrebonne, QC) with real-time kinematic centimeter-level positional accuracy. In 2019, the base locations were displaced 15 m to the east of the 2018 base locations to reduce the impacts of the previous sampling year on GHG measurements, compaction around the gas sampling base, etc.

Gas fluxes were measured using non-flow-through non-steady-state chambers composed of a chamber cover and base. The plexiglass base was 0.56 m x 0.56 m x 0.17 m (W x L x H), inserted to a depth of 5 cm. On gas sampling dates, the plexiglass chamber cover (0.565 m x 0.565 m x 0.05 m) was placed on top of the base, creating a headspace of 41.71 L. The bottom of the chamber cover was lined with closed cell insulating foam tape (1.3 cm, Climaloc, Mississauga, ON) to create an airtight seal between the top of the base and the bottom of the chamber cover. The chamber cover had a sampling tube (0.5 cm internal diameter, 15 cm long) in one corner and a ventilation tube (1.5 cm internal diameter, 30 cm long) in the opposite corner to equilibrate the pressure within the chamber with fluctuations in outside atmospheric pressure. Reflective insulation on the chamber covers reduced temperature differences between the chamber headspace and the surrounding atmosphere.

Gas fluxes were measured periodically from May to August in 2018 and June to August in 2019. Generally, the headspace gases were collected every 6-10 d, within 48 h of a major rainfall event ( $> 0.5$  mm). During a dry period from July to August 2018, the gas samples were collected every 10-15 d. Three air samples were collected to establish the atmospheric concentration of greenhouse gases, prior to sampling gas from the chamber headspace. Chamber covers were

placed on top of the base, the headspace gases were sampled after 0, 15, 30, 45 and 60 min, and then the chamber covers were removed until the next gas collection date. Gas sampling occurred between 8:00 to 14:00 to constrain the diurnal variation in gas fluxes. Headspace gas was collected using a 20 mL plastic syringe and injected into pre-evacuated 12 mL glass Exetainer™ (Labco, High Wycombe, UK) with double wadded septa.

The N<sub>2</sub>O, CO<sub>2</sub> and CH<sub>4</sub> concentration in gas was analyzed with a Bruker 450 gas chromatograph (Bruker Corporation, Billerica, MA, USA) within 14 d of sample collection. The gas chromatograph uses an electron captor detector (operating at 350 °C) and a flame ionization detector (operating at 300 °C). Two field air samples (collected at the same time and location of chamber sampling) and two gas control samples (a. 0.34 ppm N<sub>2</sub>O, 1.19 ppm of CH<sub>4</sub>, 346 ppm of CO<sub>2</sub> and b. 1.09 ppm N<sub>2</sub>O, 3.03 ppm CH<sub>4</sub>, 990 ppm CO<sub>2</sub>) were included with each batch of field sampled exetainers.

### *3.2.4 Gas flux calculations and seasonal emissions*

Flux of N<sub>2</sub>O ( $\mu\text{g N}_2\text{O-N m}^{-2} \text{ min}^{-1}$ ) and flux of CO<sub>2</sub> ( $\mu\text{g CO}_2\text{-C m}^{-2} \text{ min}^{-1}$ ) were determined for each chamber on each sampling date, based on five headspace gas samples (0, 5, 10, 20 and 30 min after placing the chamber cover), with the HMR package (v1.0.0, Pedersen, 2019), in the statistical software R (version i386 3.4.1, Comprehensive R Archive Network, Vienna, Austria), was used to calculate the gas fluxes of N<sub>2</sub>O and CO<sub>2</sub> ( $F_{HMR}$ ). The flux calculation method, linear, non-linear (HMR) or no flux, was selected on the recommendation of the HMR package. Fluxes were assumed to be valid if there was a gradual increase in CO<sub>2</sub> concentration in the headspace from 0 to 30 min after placing the chamber cover. If the CO<sub>2</sub> concentration oscillated or

decreased with time after placing the chamber cover, the data was manually evaluated to determine if this was due to the presence of outliers or data errors. We removed outliers, e.g., 60 min measurements lower than the 0 min measurement when all chamber concentrations were increasing after 0 min, before re-analyzing the CO<sub>2</sub> and N<sub>2</sub>O flux from  $n < 5$  data points with the HMR package. There were 92 outliers among the 4800 timepoints in the gas flux database. The HMR flux ( $F_{HMR}$ ) was corrected with the daily air pressure value according to Rochette & Bertrand (2007) where

$$F = F_{HMR} \left(1 - \frac{ep}{p}\right)$$

where:

$F$  = corrected gas flux ( $\mu\text{g N}_2\text{O-N m}^{-2} \text{ min}^{-1}$  or  $\mu\text{g CO}_2\text{-C m}^{-2} \text{ min}^{-1}$ )

$F_{HMR}$  = HMR flux value

$ep$  = average partial pressure of water vapor (kPa)

$p$  = average station pressure (kPa)

The  $ep$  and  $p$  for each chamber was based on the average pressure measured in 2 representative chambers (designated at random) during each headspace sampling period with a Kestrel Drop D3 (Kestrel Meters, Boothwyn, PA) data logging device. Cumulative emissions of N<sub>2</sub>O ( $\text{mg N}_2\text{O-N m}^{-2}$ ) and CO<sub>2</sub> ( $\text{g CO}_2\text{-C m}^{-2}$ ) were calculated using linear interpolation between sampling dates.

### *3.2.5 Ancillary measurements*

Weather conditions were monitored from May to October (2018 and 2019) with a HOBO<sup>®</sup> RX3000 (Onset Computer Corporation, Bourne, MA) weather monitoring station located in the experimental field. Cloud-based data from this station provided hourly summaries of air temperature (°C), rain (mm), solar radiation (W/m<sup>2</sup>), wind speed (m/s), gust speed (m/s), relative humidity (%), dew point (°C) and wind direction. Soil temperature ( $\pm 1^\circ\text{C}$ ) and moisture ( $\pm 3\%$  volumetric water content) were measured using Decagon 5TM (METER Group, Inc., Pullman, WA) soil probes, placed 10-15 cm into the soil, at each gas sampling base location. Data was collected each hour onto a SD card using a programmed Arduino (Arduino, Somerville, MA). Changes in temperature, moisture and pressure in the gas chamber were evaluated with a Kestrel Drop D3 (Kestrel Meters, Boothwyn, PA) device placed into one chamber at random on each sampling day.

### *3.2.6 Soil sampling and analysis*

Soil was collected on the same date as the gas sampling. Soil samples were collected within 2.0 m of the gas sampling chamber (n=3, 0-20 cm depth) after removing excess surface vegetation. Soil samples (3 per chamber location) were taken with a 2 cm diameter probe and mixed together to make a composite sample (~ 250 g). Following 2 M KCl extraction (1:10 soil: extractant), the soil solution was analyzed for  $\text{NH}_4^+$  and  $\text{NO}_3^-$  using a Lachat QuikChem<sup>®</sup> 8500 Series 2 Flow Injection Analysis System (Hatch, Loveland, CO).

End-of-season soil sampling was completed in October 2018 and October 2019. To avoid confounding effects, locations of the end-of-season soil sampling points were randomly assigned

within a grid using ArcGIS in 2018 and 2019 so that different locations were sampled in each year. Five to ten soil cores were collected randomly within a 2 m radius of the target sampling location within each fertilizer treatment in the zone, at least 1.5 m from the edge of the strip that received fertilizer. To represent the soil conditions in the vicinity of the gas sampling chamber, we also collected soil within 2.0 m of each gas sampling location.

### *3.2.7 Plant sampling and analysis during the growing season*

Switchgrass foliage was sampled at the same time as gas samples. We removed the second fully formed leaf below the apical growing point, and 30 leaves were collected from switchgrass plants around each GHG sampling location. Leaves always came from a plant that was never sampled previously, verified by looking at the plant stem for missing leaves. Leaf biomass was determined by drying to a constant mass (oven-dried at 70 °C for 24 h). Then, leaf samples were ground (<1 mm), digested in sulfuric acid (Isaac & Johnson, 1976) and analyzed for total N concentration (g N kg<sup>-1</sup> plant tissue) with a Lachat QuikChem<sup>®</sup> 8500 Series 2 Flow Injection Analysis System (Hatch, Loveland, CO).

End of season biomass sampling was completed in October 2018 and October 2019. Sampling points were chosen at random from a grid that included one sampling point within 20 m of the center of the strip, at least 1.5 m from edge of the strip. A second sampling point was selected randomly within 2.0 m of each gas sampling location (Fig. 3-1). Sampling points were located with a GPS with RTK functionality (accuracy of ±0.5 m). The GPS-located point was the south-west corner of a 1 m<sup>2</sup> quadrant where switchgrass biomass was recorded. The maximum plant height (m) was determined with a measuring tape attached to a pole, then the switchgrass

was cut as close to the surface as possible (on average, 5.0 cm above the soil surface). Biomass was weighed on a bucket ElectroSamson Digital Handheld Scale (Brecknell, Montreal, QC) before a 500 g sub-sample was taken to evaluate the moisture content (oven-dried at 70 °C to constant mass).



**Figure 3-1.** Map of the experimental switchgrass field, showing the treatment blocks and location of biomass and soil sampling points.

### 3.2.8 Statistical analysis

In the 2018 and 2019 sampling seasons, Shapiro-Wilk normality tests concluded that N<sub>2</sub>O cumulative emissions were non-normal. Differences in soil N<sub>2</sub>O and CO<sub>2</sub> daily fluxes were evaluated with the Kruskal-Wallis test at the 0.05 alpha level.

## 3.3 Results

### 3.3.1 Gas emissions

In the 2018 sampling season, the peak CO<sub>2</sub> fluxes occurred on the same days in each fertilizer treatment in Zone 1 and Zone 3 after fertilizer application, on Julian day 180 and on Julian day 205 (Fig. 3-2). Peak N<sub>2</sub>O flux measurements occurred within 2 wk after fertilizer application and gradually decreased to ~0 mg N<sub>2</sub>O-N m<sup>-2</sup> d<sup>-1</sup> by Julian day 173 in 2018 (Fig. 3-3). In 2018, there was a tendency for increasing N<sub>2</sub>O flux from Julian day 180 to the end of the growing season in plots that received 0 kg N ha<sup>-1</sup> (Fig. 3-3). In the 2019 season, the peak CO<sub>2</sub> flux was on Julian day 186, which was 17 d after fertilizer application, and declined consistently in all fertilizer treatments and both zones for the rest of the growing season (Fig. 3-4). Peak N<sub>2</sub>O fluxes occurred on Julian day 179, which was 10 d after fertilizer application, for all fertilizer treatments in both zones (Fig. 3-5). By Julian day 186, the flux was < 2 mg N<sub>2</sub>O-N m<sup>-2</sup> d<sup>-1</sup> and fluxes remained between 0 and 2 mg N<sub>2</sub>O-N m<sup>-2</sup> d<sup>-1</sup> until the end of the sampling seasons (Fig. 3-5).

In 2018, the Kruskal-Wallis test results showed that there were differences in N<sub>2</sub>O in the N-fertilized strips compared to the control on the first two flux sampling dates (n=24, P > 0.05),

Julian day 153 and 157. In 2019, the Kruskal-Wallis test results showed that there were differences in CO<sub>2</sub> in the N-fertilized strips compared to the control on the third day, 166, of flux sampling (n=24, P > 0.05).

Cumulative growing season emissions were calculated for each chamber in 2018 (Table 3-1) and 2019 (Table 3-2). The linear regression analysis of cumulative CO<sub>2</sub> and N<sub>2</sub>O growing season emissions trendlines showed that there was only a significant difference between Zone 1 and Zone 3 in 2018 (Table 3-3, Fig. 3-6). This is likely due to the lower N fertilizer rates in 2018 and the high rates of N fertilizer application in 2019.

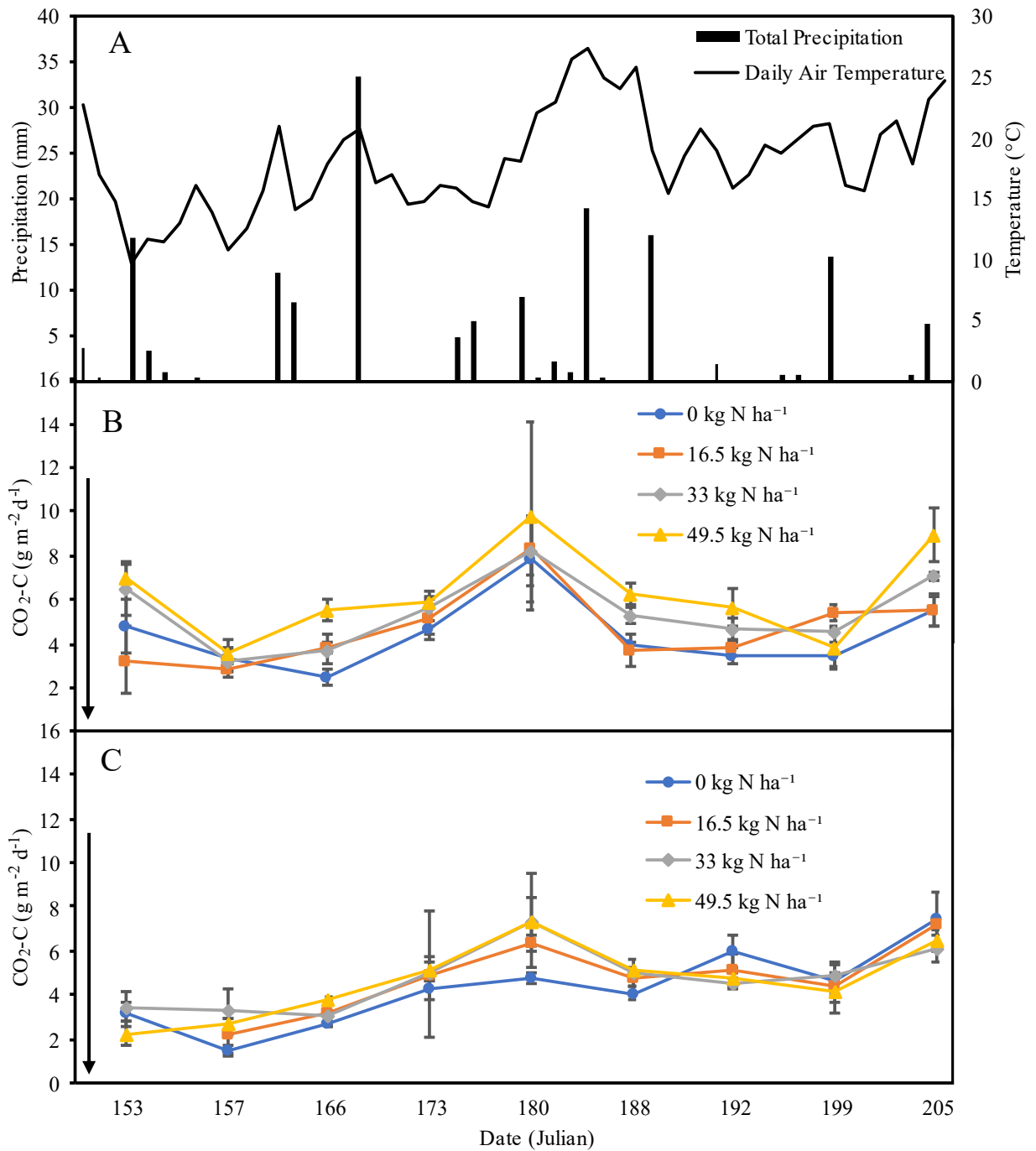


**Figure 3-2.** Weather data for the A: 2018 sampling season. Total daily precipitation (mm) is represented by black bars. Average daily temperature (°C) is represented by the black line. Mean CO<sub>2</sub> flux time series in B: Zone 1 and C: Zone 3 on every sampling day during the 2018 sampling season. Error bars are  $\pm$ SEM (n=3). The N fertilizer was applied on Julian day 151 (May 31, 2018), indicated by the black arrow.

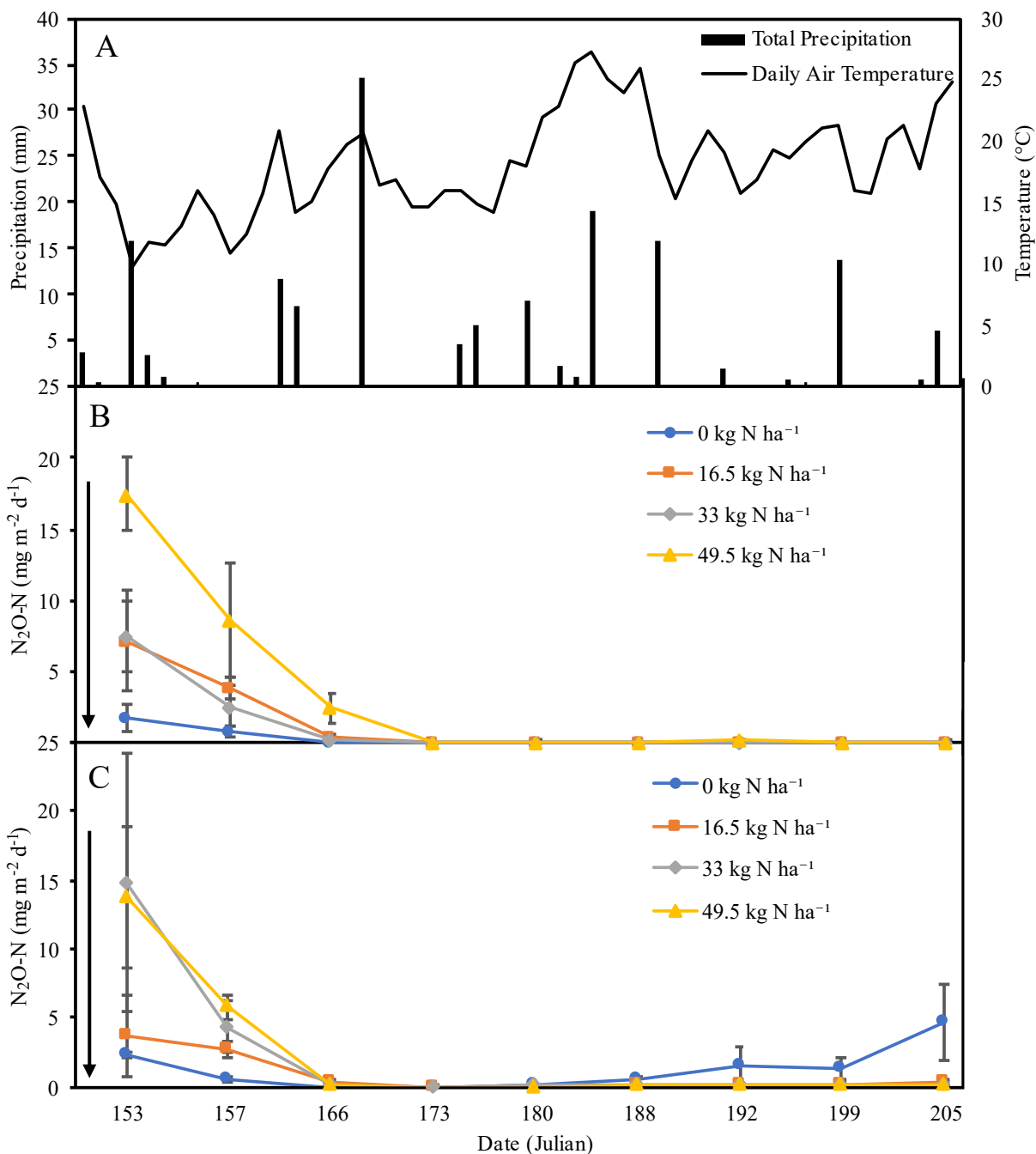


**Figure 3-3.** Weather data for the A: 2018 sampling season. Total daily precipitation (mm) is represented by black bars. Average daily temperature (°C) is represented by the black line. Mean N<sub>2</sub>O flux time series in B: Zone 1 and C: Zone 3 on every sampling day during the 2018 sampling season. Error bars are ±SEM (n=3). The N fertilizer was applied on Julian day 151 (May 31, 2018), indicated by the black arrow.

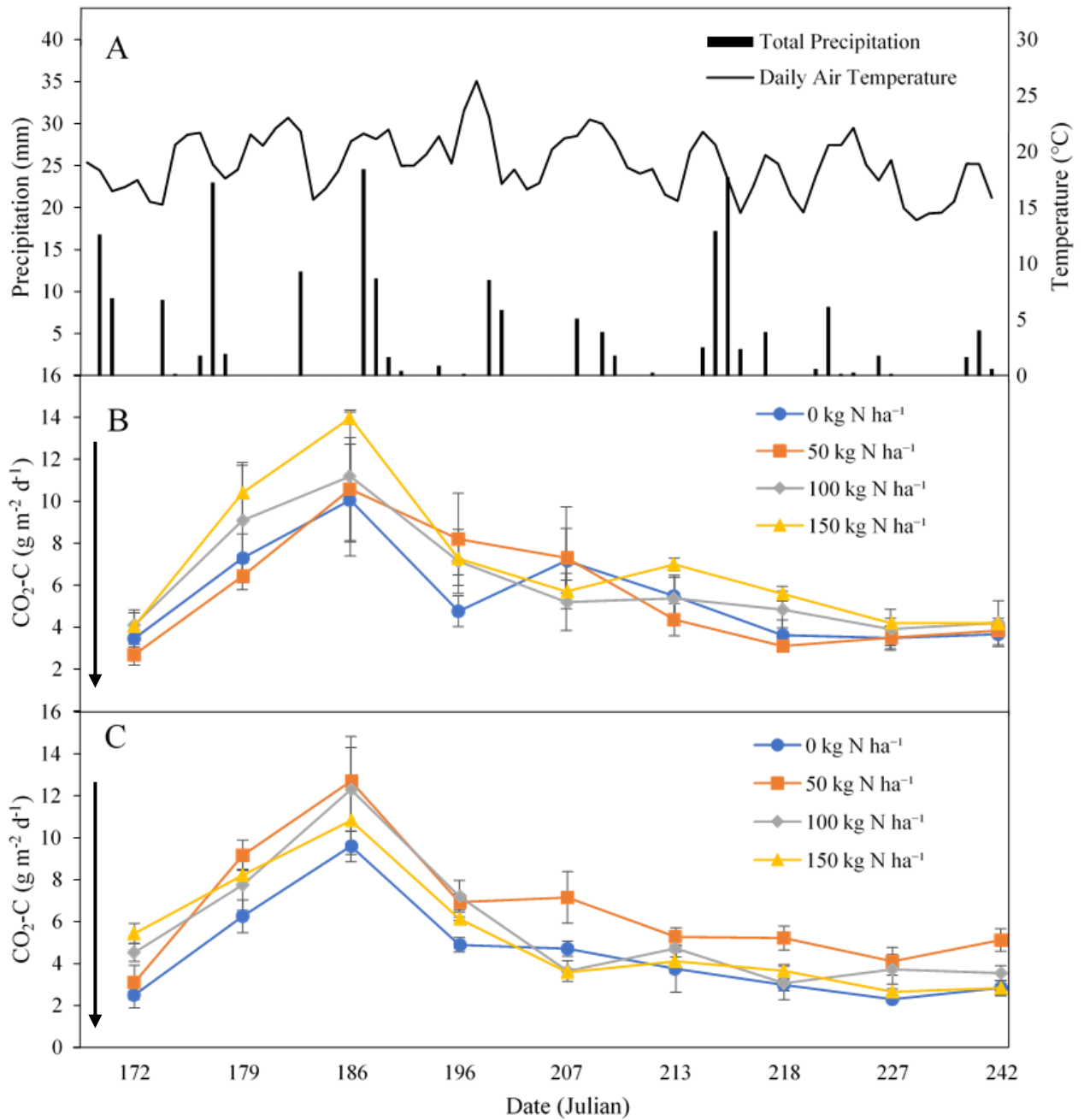


**Figure 3-4.** Weather data for the A: 2019 sampling seasons. Total daily precipitation (mm) is represented by black bars. Average daily temperature (°C) is represented by black line. Mean CO<sub>2</sub> flux time series in B: Zone 1 and C: Zone 3 on every sampling day during the 2019 sampling season. Error bars are ±SEM (n=3). The N fertilizer was applied on Julian day 169 (June 18, 2019), indicated by the black arrow.

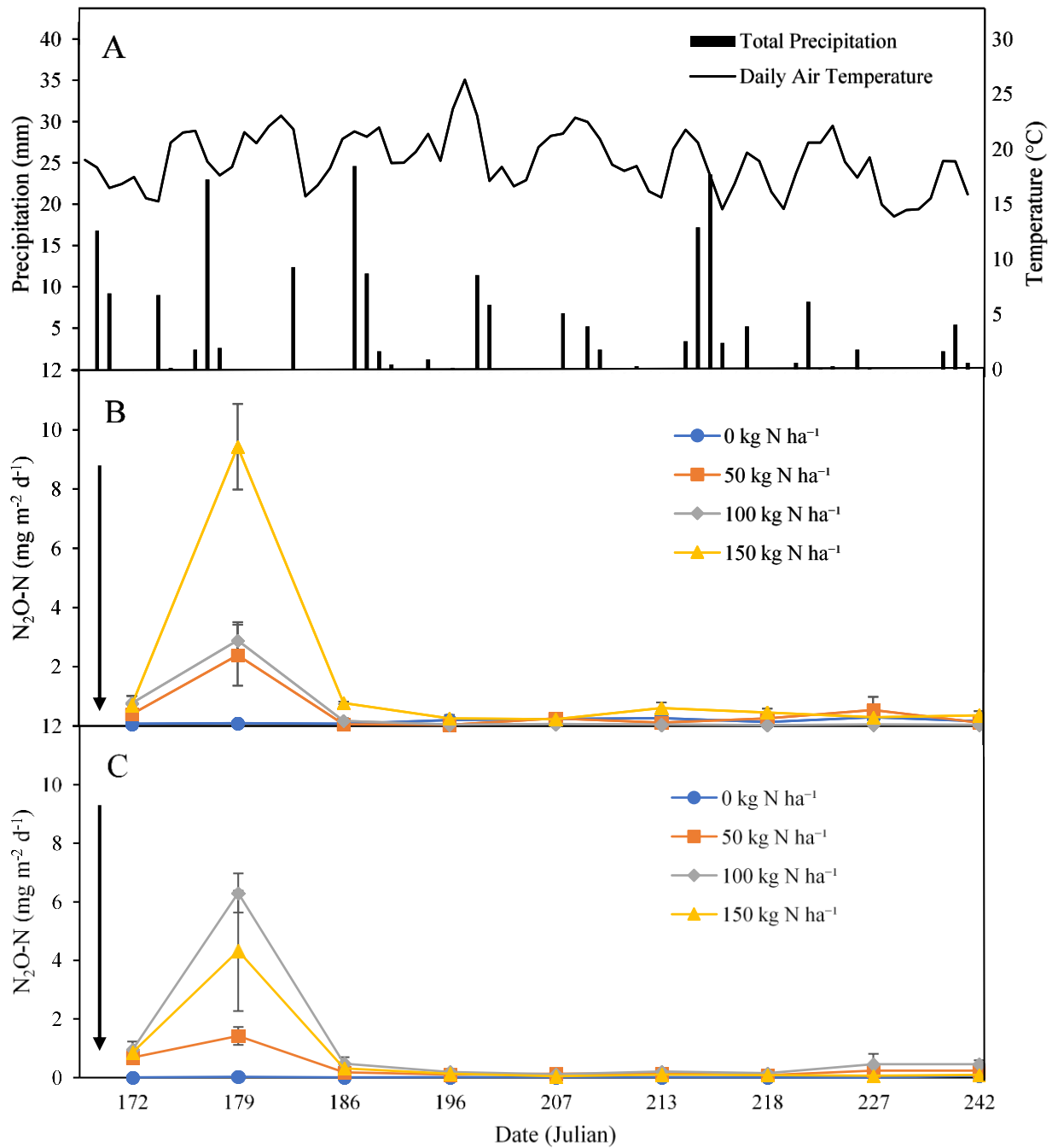


**Figure 3-5.** Weather data for the A: 2019 sampling seasons. Total daily precipitation (mm) is represented by black bars. Average daily temperature (°C) is represented by the black line. Mean N<sub>2</sub>O flux time series in B: Zone 1 and C: Zone 3 on every sampling day during the 2019 sampling season. Error bars are  $\pm$ SEM (n=3). The N fertilizer was applied on Julian day 169 (June 18, 2019), indicated by the black arrow.

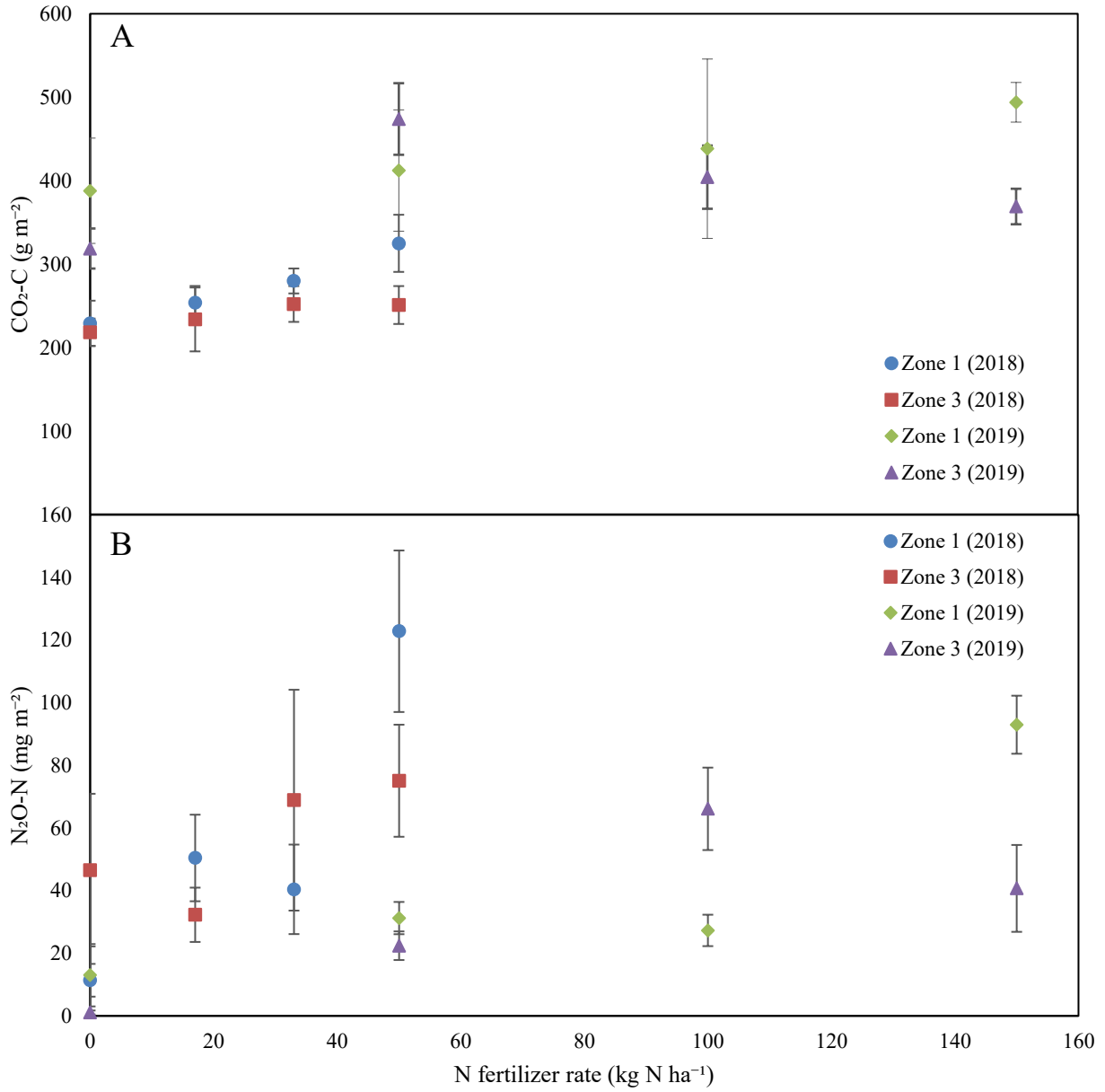


**Figure 3-6.** Cumulative seasonal emissions of A: CO<sub>2</sub> and B: N<sub>2</sub>O from switchgrass plots in the 2018 and 2019 seasons. Points are the average of n=3 measurements per zone, and error bars are ±SEM.

**Table 3-1.** Cumulative growing season emissions in 2018, presented as the interpolated cumulative values  $\pm$  SEM, n=24.

Zone	Fertilizer Rate (kg N ha <sup>-1</sup> )	Chamber	N <sub>2</sub> O-N (mg m <sup>-2</sup> )	CO <sub>2</sub> -C (g m <sup>-2</sup> )
1	0	22	21.1 $\pm$ 0.11	199 $\pm$ 0.14
	0	23	9.73 $\pm$ 0.04	206 $\pm$ 0.14
	0	24	3.26 $\pm$ 0.01	283 $\pm$ 0.33
	17	19	72.5 $\pm$ 0.36	240 $\pm$ 0.15
	17	20	25.0 $\pm$ 0.11	293 $\pm$ 0.31
	17	21	53.8 $\pm$ 0.29	228 $\pm$ 0.17
	33	7	69.0 $\pm$ 0.39	280 $\pm$ 0.32
	33	8	25.2 $\pm$ 0.17	254 $\pm$ 0.15
	33	9	27.1 $\pm$ 0.11	306 $\pm$ 0.15
	50	10	78.6 $\pm$ 0.56	318 $\pm$ 0.16
	50	11	168 $\pm$ 0.72	269 $\pm$ 0.20
	50	12	122 $\pm$ 0.56	387 $\pm$ 0.51
3	0	16	26.4 $\pm$ 0.09	188 $\pm$ 0.13
	0	17	95.1 $\pm$ 0.33	244 $\pm$ 0.25
	0	18	18.2 $\pm$ 0.08	222 $\pm$ 0.24
	17	13	49.3 $\pm$ 0.25	210 $\pm$ 0.19
	17	14	20.8 $\pm$ 0.10	183 $\pm$ 0.15
	17	15	26.7 $\pm$ 0.14	309 $\pm$ 0.33
	33	1	139 $\pm$ 0.90	210 $\pm$ 0.17
	33	2	28.8 $\pm$ 0.24	282 $\pm$ 0.23
	33	3	38.7 $\pm$ 0.19	265 $\pm$ 0.17
	50	4	111 $\pm$ 0.69	247 $\pm$ 0.17
	50	5	60.6 $\pm$ 0.34	214 $\pm$ 0.14
	50	6	54.0 $\pm$ 0.25	292 $\pm$ 0.31

**Table 3-2.** Cumulative growing season emissions in 2019, presented as the interpolated cumulative values  $\pm$  SEM, n=24.

Zone	Fertilizer Rate (kg N ha <sup>-1</sup> )	Chamber	N <sub>2</sub> O-N (mg m <sup>-2</sup> )	CO <sub>2</sub> -C (g m <sup>-2</sup> )
1	0	22	32.8 $\pm$ 0.02	375 $\pm$ 0.23
	0	23	4.45 $\pm$ 0.0	503 $\pm$ 0.34
	0	24	1.67 $\pm$ 0.0	286 $\pm$ 0.17
	50	19	35.7 $\pm$ 0.13	553 $\pm$ 0.49
	50	20	37.1 $\pm$ 0.06	311 $\pm$ 0.15
	50	21	21.0 $\pm$ 0.03	372 $\pm$ 0.28
	100	7	37.3 $\pm$ 0.12	238 $\pm$ 0.11
	100	8	23.1 $\pm$ 0.06	606 $\pm$ 0.39
	100	9	21.5 $\pm$ 0.07	470 $\pm$ 0.31
	150	10	105 $\pm$ 0.29	541 $\pm$ 0.38
	150	11	99.4 $\pm$ 0.31	467 $\pm$ 0.32
	150	12	74.7 $\pm$ 0.19	473 $\pm$ 0.32
	3	0	16	0.457 $\pm$ 0.00
0		17	2.37 $\pm$ 0.00	275 $\pm$ 0.20
0		18	0.44 $\pm$ 0.00	323 $\pm$ 0.27
50		13	29.0 $\pm$ 0.05	541 $\pm$ 0.34
50		14	13.6 $\pm$ 0.04	394 $\pm$ 0.23
50		15	24.7 $\pm$ 0.04	486 $\pm$ 0.32
100		1	58.5 $\pm$ 0.18	342 $\pm$ 0.21
100		2	91.8 $\pm$ 0.20	473 $\pm$ 0.44
100		3	48.1 $\pm$ 0.14	397 $\pm$ 0.32
150		4	36.5 $\pm$ 0.09	335 $\pm$ 0.24
150		5	19.1 $\pm$ 0.05	408 $\pm$ 0.37
150		6	66.6 $\pm$ 0.24	364 $\pm$ 0.30

**Table 3-3.** Linear regression of cumulative growing season emissions, in relation to the N fertilizer rate. The slope and intercept of the best-fit line ( $\pm$  SEM) were calculated with R statistical software.

Gas	Year	Zone	Linear Equation
CO <sub>2</sub> -C (g m <sup>-2</sup> )	2018	1	CO <sub>2</sub> flux = 1.89 ( $\pm$ 0.20) $\times$ N fertilizer + 225 ( $\pm$ 6.34)
		3	CO <sub>2</sub> flux = 0.70 ( $\pm$ 0.19) $\times$ N fertilizer + 221 ( $\pm$ 5.89)
	2019	1	CO <sub>2</sub> flux = 0.69 ( $\pm$ 0.11) $\times$ N fertilizer + 381 ( $\pm$ 9.98)
		3	CO <sub>2</sub> flux = 0.16 ( $\pm$ 0.71) $\times$ N fertilizer + 379 ( $\pm$ 66.0)
N <sub>2</sub> O-N (mg m <sup>-2</sup> )	2018	1	N <sub>2</sub> O flux = 1.96 ( $\pm$ 0.72) $\times$ N fertilizer + 7.17 ( $\pm$ 22.3)
		3	N <sub>2</sub> O flux = 0.73 ( $\pm$ 0.40) $\times$ N fertilizer + 37.4 ( $\pm$ 12.5)
	2019	1	N <sub>2</sub> O flux = 0.47 ( $\pm$ 0.20) $\times$ N fertilizer + 5.72 ( $\pm$ 18.6)
		3	N <sub>2</sub> O flux = 0.33 ( $\pm$ 0.20) $\times$ N fertilizer + 8.20 ( $\pm$ 18.4)

### 3.3.2 Biomass and ancillary measurements

In 2018, soil NO<sub>3</sub><sup>-</sup> and NH<sub>4</sub><sup>+</sup> peaked within 30 d after N fertilizer application in both zones, with 0 to 15 mg NO<sub>3</sub><sup>-</sup> kg<sup>-1</sup> and 0 to 20 mg NH<sub>4</sub><sup>+</sup> kg<sup>-1</sup> during the growing season (Fig. 3-7). In 2018, NO<sub>3</sub><sup>-</sup> values remained between 0 and 15 mg NO<sub>3</sub><sup>-</sup> kg<sup>-1</sup> and NH<sub>4</sub><sup>+</sup> remained between 0 and 20 mg NH<sub>4</sub><sup>+</sup> kg<sup>-1</sup>. In 2019, NO<sub>3</sub><sup>-</sup> values were between 0 and 2 mg NO<sub>3</sub><sup>-</sup> kg<sup>-1</sup> in both zones (Fig. 3-8). In 2019, NH<sub>4</sub><sup>+</sup> peaked after fertilizer application and stayed between 0 and 15 mg NH<sub>4</sub><sup>+</sup> kg<sup>-1</sup> 20 d after fertilization.

In 2018, switchgrass biomass at the end of the growing season tended to be greater in Zone 1 than Zone 3 (Table 3-4). Biomass N concentrations were higher in the early part of the growing season and declined with time, in both years of the study, probably due to a dilution effect as the switchgrass accumulated more carbon/ dry matter relative to its nitrogen requirements (Fig. 3-8, Fig. 3-9, Fig. 3-10).

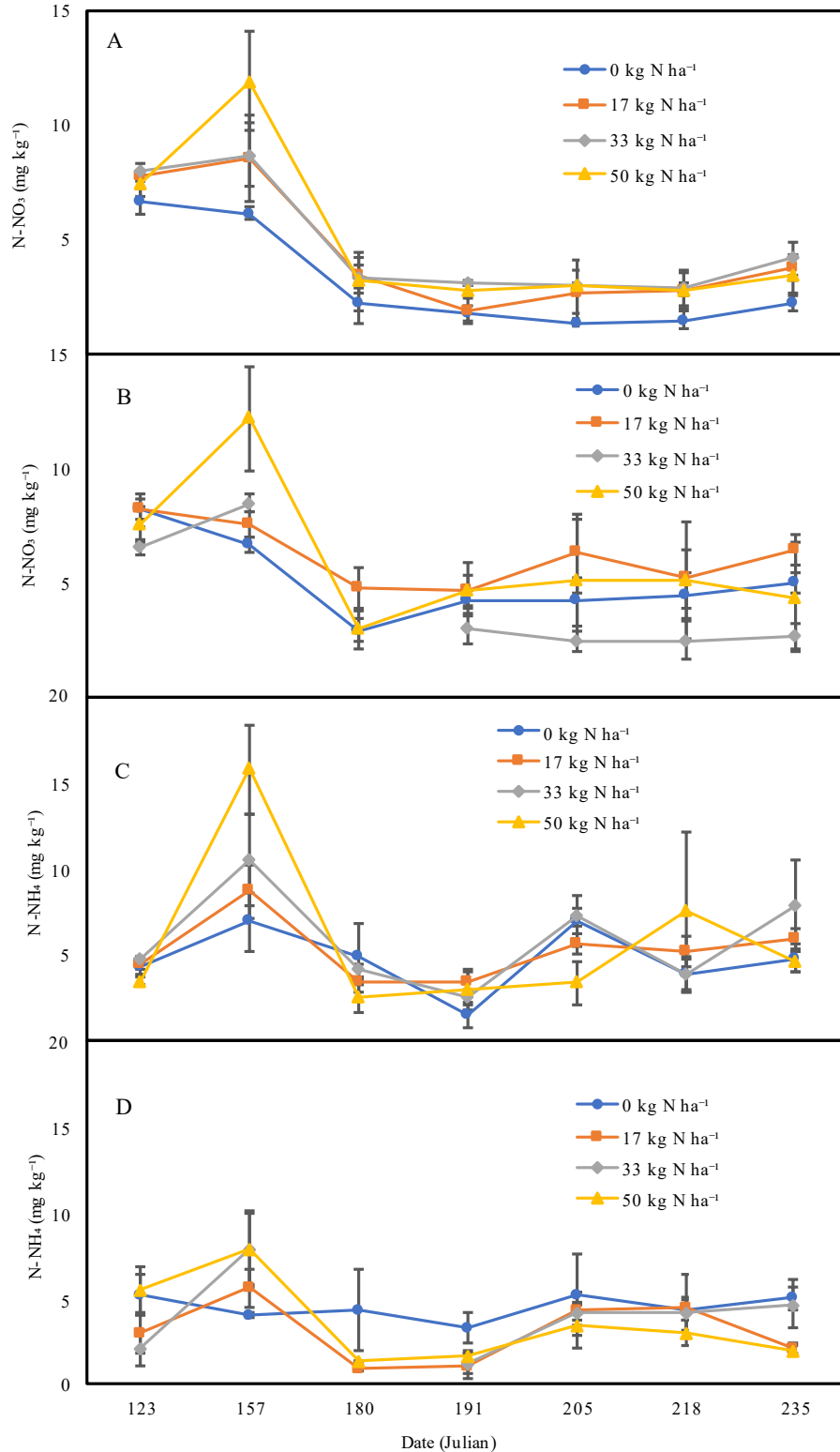


**Figure 3-7.** Average soil NH<sub>4</sub><sup>+</sup> and NO<sub>3</sub><sup>-</sup> concentrations for each fertilizer application rate in 2018 of A: Zone 1 NO<sub>3</sub><sup>-</sup>, B: Zone 3 NO<sub>3</sub><sup>-</sup>, C: Zone 1 NH<sub>4</sub><sup>+</sup>, D: Zone 3 NH<sub>4</sub><sup>+</sup>. Fertilizer applied on 151 (May 31, 2018). Points are the mean (n=3) with ±SEM bars.

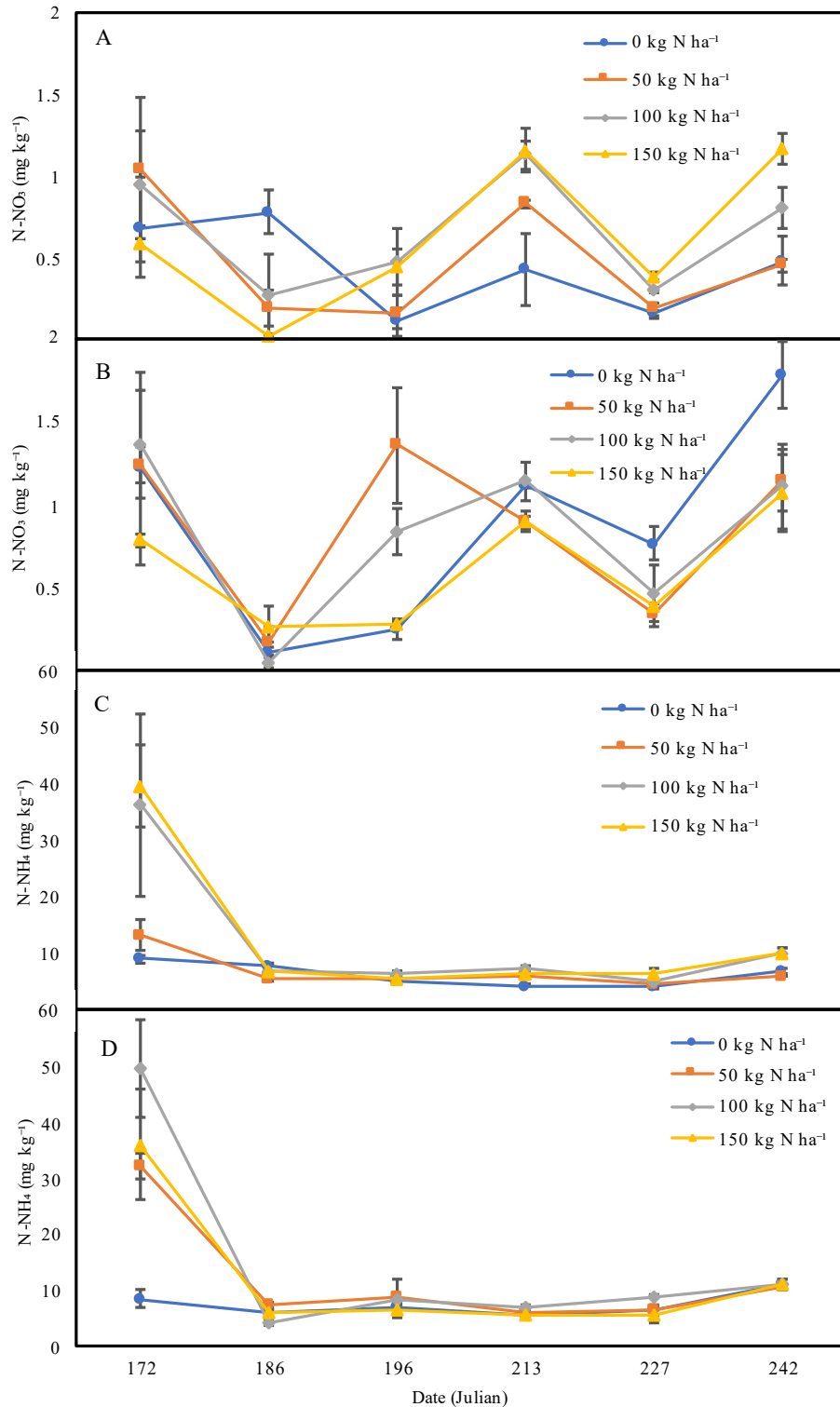


**Figure 3-8.** Average soil NH<sub>4</sub><sup>+</sup> and NO<sub>3</sub><sup>-</sup> concentrations for each fertilizer application rate in 2019 of A: Zone 1 NO<sub>3</sub><sup>-</sup>, B: Zone 3 NO<sub>3</sub><sup>-</sup>, C: Zone 1 NH<sub>4</sub><sup>+</sup>, D: Zone 3 NH<sub>4</sub><sup>+</sup>. Fertilizer applied on 169 (June 18, 2019). Points are the mean (n=3) with ±SEM bars.

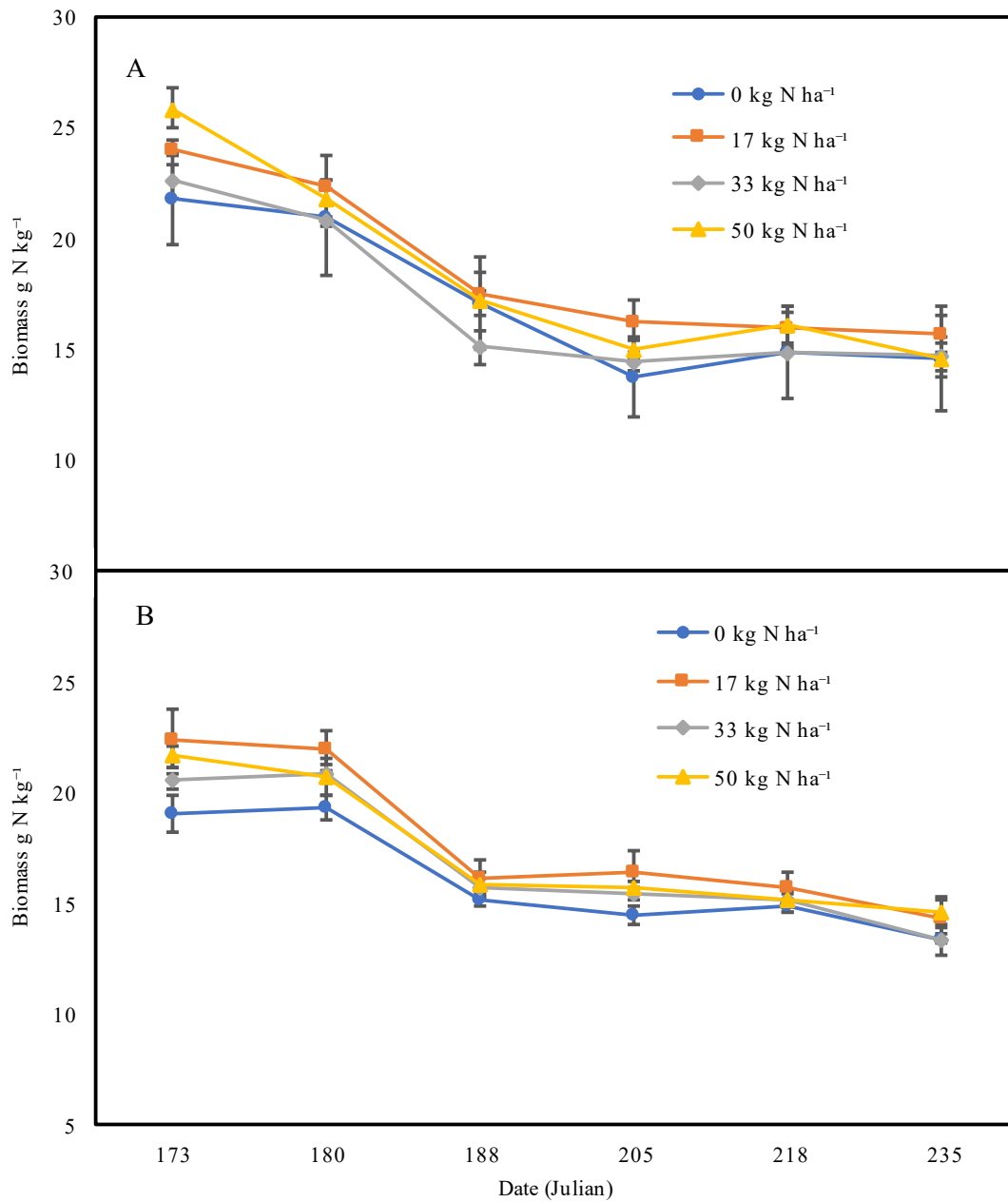


**Figure 3-9.** Average N concentration in switchgrass biomass in A: Zone 1 and B: Zone 3 during the 2018 sampling season. The N fertilizer was applied on Julian day 151 (May 31, 2018). Points are the mean (n=3) with  $\pm$ SEM bars.

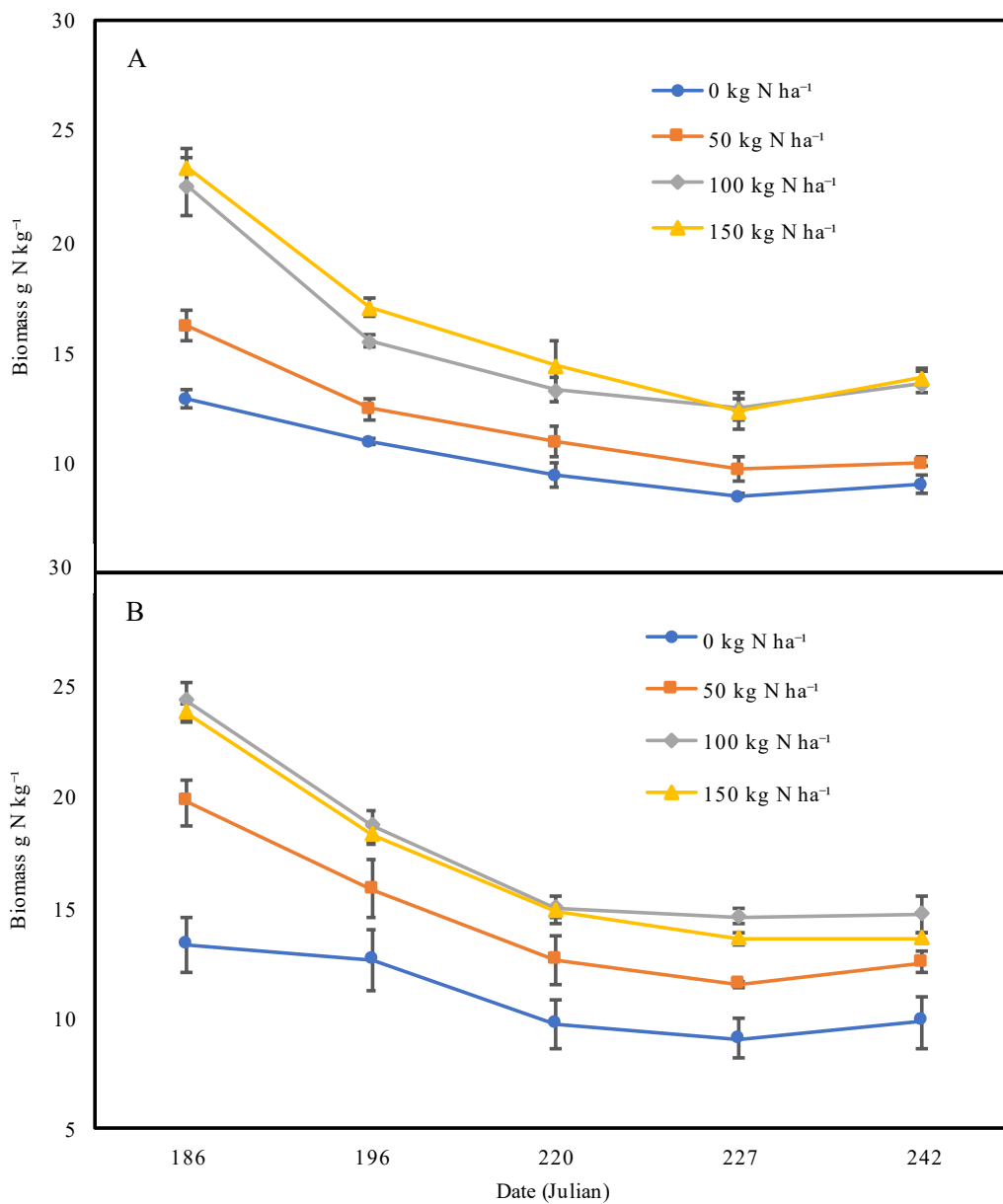


**Figure 3-10.** Average N concentration in switchgrass biomass in A: Zone 1 and B: Zone 3 during the 2019 sampling season. The N fertilizer was applied on Julian day 169 (June 18, 2019). Points are the mean (n=3) with  $\pm$ SEM bars.

**Table 3-4.** End of season above ground biomass yield (t dry matter ha<sup>-1</sup>) adjacent to the gas sampling locations. Values are the mean ± SEM, n=3.

Year	Fertilizer Rate (kg N ha <sup>-1</sup> )	Switchgrass yield (t ha <sup>-1</sup> )	
		Zone 1	Zone 3
2018	0	9.37 (± 0.57)	8.25 (± 0.49)
	17	9.36 (± 0.62)	8.35 (± 0.45)
	33	10.4 (± 1.05)	9.05 (± 0.52)
	50	12.1 (± 1.34)	9.78 (± 0.21)
2019	0	7.18 (± 1.85)	9.63 (± 1.35)
	50	7.79 (± 0.67)	9.79 (± 1.21)
	100	11.6 (± 0.81)	11.6 (± 1.03)
	150	10.3 (± 1.32)	10.8 (± 0.33)

### 3.4 Discussion

My first hypothesis, that the control of 0 kg N ha<sup>-1</sup> will have significantly lower N<sub>2</sub>O emissions than the other three fertilizer rates, was supported on some, but not all GHG sampling dates. I believe that the lack of significant differences in emissions on sampling dates later in the season happened due to the hardiness of the switchgrass crop and its ability to efficiently take up N from the soil. My second hypothesis, that that the management zone with greater soluble N concentration (due to less plant growth and higher N fertilizer rates) will produce more N<sub>2</sub>O during periods when the field is temporarily waterlogged (i.e., after rainfall), was not supported in 2019 as there was no difference in the slope of the trendlines for cumulative emissions in Zone 1 and Zone 3.

#### 3.4.1 Gas emissions and site-specific N

Most hot moments of gas flux occurred within the first 30 days following fertilizer

application for all gases in each zone and year. The only exception was CO<sub>2</sub> in 2018, where daily fluxes gradually increased from the fertilizer application date to their peak at 30 days after fertilizer application. The higher slope for cumulative emission, in Zone 1 compared to Zone 3, at increasing rates indicates that Zone 1 fertilizer rates increased emissions at a higher rate than in Zone 3. Zone 1 was initially believed to be the zone that was better suited for switchgrass growth as it was higher in elevation than Zone 3 and the producer mentioned that the historical yields in that zone were generally better than the surrounding field.

#### *3.4.2 Ancillary measurements and management zones*

In 2018, the switchgrass with the 0 kg N ha<sup>-1</sup> fertilizer application rate generally had lower total N than all other fertilizer treatment rates. In 2019, the switchgrass growing in the 0 kg N ha<sup>-1</sup> fertilizer application rate strips always had lower total N concentrations than the other treatment rates.

In 2018, average soil NO<sub>3</sub><sup>-</sup> and NH<sub>4</sub><sup>+</sup> peaked within the first 30 d after N fertilizer application (Fig. 3-7). Measurements were taken on Julian day 123, 28 d before N fertilizer application, and did not differ significantly for NH<sub>4</sub><sup>+</sup> (Fig. 3-7). Soil NO<sub>3</sub><sup>-</sup> values during the sampling season were lower than the NO<sub>3</sub><sup>-</sup> values measured before N fertilizer was applied.

In 2019, NO<sub>3</sub><sup>-</sup> appears to fluctuate, however the scale is small and NO<sub>3</sub><sup>-</sup> values remain between 0 and 2 mg NO<sub>3</sub><sup>-</sup> kg<sup>-1</sup> in both zones (Fig. 3-8). In both zones, NH<sub>4</sub><sup>+</sup> peaked after fertilizer application and remained below 15 mg NH<sub>4</sub><sup>+</sup> kg<sup>-1</sup> 20 d after fertilization for the remainder of the sampling season, which is reasonable considering that the fertilizer was the

main source of N in the field and that it was transformed and used by the switchgrass since N was no longer a limiting factor for growth.

The switchgrass yields of 7.18 to 12.1 t ha<sup>-1</sup> measured in our field were consistent with, and slightly better, than the on-farm historical yield and other yield measures of the Cave-in-Rock cultivar in southern Québec. The cooperating producer grows switchgrass and achieved yields of 5 to 11 t ha<sup>-1</sup> during the 2012 growing season (personal communication with the farmer, 2018). The highest yields achieved in our field and on this farm are superior to the average yield of 8.97 t ha<sup>-1</sup> for the Cave-in-Rock cultivar calculated at 5 experimental sites in Québec during a 4 yr period from 2013 to 2016 (Martel & Lalonde, 2018).

### **3.5 Conclusions**

The findings of this study suggest that most of the N fertilizer applied to this switchgrass field was retained in the soil-plant system, since the soil NO<sub>3</sub><sup>-</sup> and NH<sub>4</sub><sup>+</sup> concentration peaked at the beginning of the season and decreased with time during both growing seasons. Since the switchgrass was planted 10 yr before this study, I expect that it established an extensive root system that was able to absorb nutrients added in the form of urea-N fertilizer. This interpretation is supported by the fact that the major hot-moments of N<sub>2</sub>O and CO<sub>2</sub> occurred within 20 to 30 d following N fertilizer application, with relatively low fluxes of these greenhouse gases for the remainder of the growing season. With gas chambers placed 15 m apart and no extreme slopes present in the field, I am confident that the measurements within each treatment band reflect the soil-plant responses and gas fluxes in response to applied N fertilizer. Although Zone 1 and Zone 3 have distinctive soil physico-chemical properties, they were fairly consistent in their biological

outcomes. Within each growing season, there was a consistent pattern of N<sub>2</sub>O and CO<sub>2</sub> flux and cumulative emissions of these gases in Zone 1 and Zone 3. Furthermore, the dynamics of soil NH<sub>4</sub><sup>+</sup> and NO<sub>3</sub><sup>-</sup> pools and switchgrass biomass at the end of the growing season responded similarly when equivalent N fertilizer rates were applied in Zone 1 and Zone 3. This suggests that plant growth and N cycling were affected more by the environmental conditions associated with year-to-year fluctuations in weather, rather than the underlying physico-chemical variability in this large 8.9 ha switchgrass field, which already had optimal growing conditions for switchgrass. This intriguing possibility should be confirmed in farm-scale experiments on other commercial farms, considering more cropping systems, soil types and multiple sampling years to reflect a broader range of realistic growing conditions on farms.

## References

- Environment Canada. (2017). Monthly meteorological summaries for Sherbrooke.  
<https://climate.weather.gc.ca/>
- Isaac, R. A., & Johnson, W. C. (1976). Determination of total nitrogen in plant tissue, using a block digester. *Association of Official Analytical Chemists*, 59, 98–100.
- Martel, H., & Lalonde, O. (2018). Guide de Production Panic Erige. Réseau des plantes bio-industrielles du Québec.
- Rochette, P., & Bertrand, N. (2007). Soil-surface gas emissions. In M. Carter & E. Gregorich (Eds.), *Soil Sampling Methods of Analysis, Second ed.* (pp. 851-861). CRC Press.

Sehy, U., Ruser, R., & Munch, J. C. (2003). Nitrous oxide fluxes from maize fields: relationship to yield, site-specific fertilization, and soil conditions. *Agriculture, Ecosystems and Environment*, *99*, 97-111. [https://doi.org/10.1016/S0167-8809\(03\)00139-7](https://doi.org/10.1016/S0167-8809(03)00139-7)

Shcherbak, I., Millar, N., & Robertson, G. P. (2014). Global Metaanalysis of the nonlinear response of soil nitrous oxide (N<sub>2</sub>O) emissions to fertilizer nitrogen. *Proceedings of the National Academy of Sciences*, *111*(25), 9199-9204.  
<https://doi.org/10.1073/pnas.1322434111>

Schwalbert, R. A., Amado, T. J. C., Reimche, G. B., & Gebert, F. (2019). Fine-tuning of wheat (*Triticum aestivum*, L.) variable nitrogen rate by combining crop sensing and management zones approaches in southern Brazil. *Precision Agriculture*, *20*, 56-77.  
<https://doi.org/10.1007/s11119-018-9581-6>

## General Discussion

My thesis presents a case study on the use of management zones for understanding N fertilizer requirements across a switchgrass field. The reasons that management zones are preferred, compared to uniform application of fertilizer, is because the variability that occurs in all fields can affect the inherent fertility and hence the nutrient demands of the crop. I wish to avoid applying an excessively high amount of N fertilizer where it is not needed by the crop because the N fertilizer can stimulate microbial activities that produce N<sub>2</sub>O, CO<sub>2</sub> and CH<sub>4</sub>, which can result in GHG emissions from the agroecosystem.

### *Mapping with management zones*

Management zones are understudied in perennial cropping systems, relative to agroecosystems with annual crops. I found 7 peer-reviewed article publications in the past 5 yr involving switchgrass and management zones, compared to >70 peer-reviewed publications in the same period describing management zones for corn production. Despite the limited information, perennial crops like switchgrass are good candidates for management zone analysis. Generally, N fertilizer is broadcast once per season, after the snow has melted and before emergence of the switchgrass, because farm machinery passing over a field of growing switchgrass would mechanically damage the tall, dense vegetation and reduce the switchgrass yield. Therefore, management zone analysis can be a strategy for understanding the field conditions and applying a suitable amount of N fertilizer to optimize the perennial crop growth over many years.

Traditional methods of determining field variability require hundreds of soil samples and extensive geostatistical analysis, involving kriging and semi-variogram analysis. This led me to attempt to simplify the management zone delineation process, based on an example that used proximal soil sensing, i.e., apparent electrical conductivity and pre-existing knowledge of the high yielding zones in the field to characterize field heterogeneity (Longchamps & Khosla, 2017). I also found that zone classification overlapped in maps that were generated with numerous ( $\geq 10$ ) variables and when the same area was mapped with half as many variables that were selected due to their importance for the growth of the crop. This indicates my method using proximal soil sensing rather than conventional soil testing data is a robust way to segregate a heterogeneous 8.9 ha field into three clearly-defined management zones. I judge the method to be ‘robust’ because of the high degree of overlap in the management zones (from 58-87% similarity) when I compared the two mapping approaches (i.e., conventional soil testing vs. proximal soil sensing).

I created field maps with Management Zone Analyst, which requires specific information and training. For instance, the agronomic decision maker who wishes to create a similar map needs access to georeferenced data to use the software and therefore must have some basic understanding of how to collect, organize and verify the accuracy of the data that will be used to create the map. Additionally, Management Zone Analyst assigns arbitrary ordinary numbers for the zone classifications so the decision maker for the field must use ArcGIS or QGIS to project the software output and compare maps generated with each data source to visualize the zones (Fridgen et al., 2004). The decision maker must also consider what variables are to be included for management zone delineation, based on some prior knowledge. The issue is that Management Zone Analyst can use any values for the clustering algorithm and some variables

are intercorrelated (i.e., they describe the same physicochemical property of the field). Providing too much information to the software could cause unimportant variables to skew the results.

### *Emission of N<sub>2</sub>O*

In both sampling years, the peak N<sub>2</sub>O flux occurred within 30 d after N fertilizer was applied. Furthermore, soil NO<sub>3</sub><sup>-</sup> and NH<sub>4</sub><sup>+</sup> concentration peaked early in the growing season, which suggests the N fertilizer applied to the field was the main source of N<sub>2</sub>O emitted from the field. The N<sub>2</sub>O emission trendlines were different in Zone 1 and Zone 3 during the 2018 growing season, indicating a site-specific variability in the N<sub>2</sub>O production and loss across the field. However, this effect was not observed during the 2019 growing season, which used higher N fertilizer rates than 2018. I deduce that the similarity in N<sub>2</sub>O emissions between Zone 1 and Zone 3 meant that environmental conditions were more favorable for switchgrass growth in 2019, with more precipitation measured at the field during the gas sampling period, and thus the crop was more efficient at using the N fertilizer. However, switchgrass yield was only 2.5% greater, on average, in 2019 than 2018.

Gas fluxes were measured with non-flow-through non-steady-state chambers, which is a cost-effective tool to measure gas fluxes in the field and interpolating the GHG emissions during the growing season. Still, the chambers cover a relatively small area (<1 m<sup>2</sup>) relative to the size of the management zones (222,000 m<sup>2</sup>) and fertilizer strip within each zone (1,500 m<sup>2</sup>). Some locations had more vegetative growth within and surrounding the gas chambers, which probably reduced the amount of GHG emitted. One way to improve the accuracy of the gas fluxes is to increase the number of chambers in the field to account for microvariability in the field.

Furthermore, N<sub>2</sub>O is produced through three separate biological processes (i.e., ammonia oxidation, nitrifier-denitrification, denitrification), depending on substrate availability, microbial activity and environmental conditions. In the future, I would recommend advanced N isotope tracing methods, using equipment like a Picarro G5131-i isotopic and gas concentration analyzer that can simultaneously measure the site specific and bulk  $\delta^{15}\text{N}$  and  $\delta^{18}\text{O}$  in N<sub>2</sub>O to discern the source of N<sub>2</sub>O emissions real-time in the field.

### *Recommendations*

My research suggests that proximal soil sensing data is suitable to represent field heterogeneity in agricultural landscapes. Future research on site-specific N fertilization could be based on non-invasive and cost-effective measurements of proximal soil sensing data, including free images of bare soil that may be obtained without charge from Google Earth and other remote sensing platforms. While my work reveals that N<sub>2</sub>O flux from a switchgrass field is related in part to N fertilizer application, this factor explains a relatively small proportion of the N<sub>2</sub>O emissions. Consequently, it is important to monitor precipitation and temperature at the field scale to understand hot spots and hot moments of organisms' activity and of emission of GHGs. Management zones might be more effective at reducing N<sub>2</sub>O emissions in annual cropping systems, but the perennial switchgrass that I studied was planted in 2008 and thus was established for 10 yr before the GHG emissions were measured. Additionally, historical yields in this switchgrass field are similar to the average switchgrass crop yield in the region (Martel & Lalonde, 2018), meaning that the producer has already optimized all of the agronomic practices that affect nutrient acquisition and growth of their switchgrass crop. In the future, I could implement a similar study in a switchgrass field that has below-average yields, meaning that it is

not using nutrients efficiently and thus will probably benefit from site-specific N fertilizer applications, which need to be calibrated to avoid N<sub>2</sub>O emissions.

## General Conclusions

Crop yield is generally uneven in agricultural fields, due to the underlying heterogeneity in soil fertility and water availability across sloping fields. Areas within the field with high crop yield may use fertilizer nutrients more efficiently than in the regions where crop growth is limited by lack of water or soil constraints. The case study for this thesis was an 8.9 ha switchgrass field in southeastern Québec with well-documented heterogeneity in yield (from 5 to 11 t ha<sup>-1</sup> across the field). Hence, the field was a good candidate for testing of precision agriculture principles. The global objective of this work was to operationally define management zones that would receive variable rates of N fertilizer, and to assess which of the N fertilizer rates applied to these management zone would support the switchgrass yield target without increasing N<sub>2</sub>O losses.

In Chapter 2, I looked at management zones and compared how a variety of data sources that could describe field heterogeneity, such as soil texture, electrical conductivity, soil surface reflectance, etc., would delineate zones. Regardless of the data source and quantity of inputs Management Zone Analyst determined that 3 management zones was reasonable, based on the normalized classification entropy and fuzziness performance index, for my research field. Proximal soil sensing data appears to be a reasonable indicator for characteristics measured by conventional soil testing. This is probably due to the fact that proximal measurements of soil ECa are correlated with soil moisture, soil organic matter, salinity and cation exchange capacity (Yari et al., 2017; Moral & Serrano, 2019). Additionally, multispectral imagery is a form of proximal soil sensing data that I found to be another good indicator of field heterogeneity. My findings were in agreement with existing literature that found multispectral imagery to be related

to soil characteristics such as soil moisture and soil C (Chen et al., 2000; Flemming et al., 2004; Georgi et al., 2018).

In Chapter 3, I studied how management zones and fertilizer application influence the emissions of GHGs and crop yields. The slopes for the trend of emission for Zone 1 and Zone 3 was different in 2018, when the N fertilizer rates were lower than the recommended rate for switchgrass, but in general the two management zones emitted a similar amount of N<sub>2</sub>O and other GHGs. The switchgrass growing in the 0 kg N ha<sup>-1</sup> fertilizer application rate strips had lower total N than all other fertilizer application rate strips in both years. In 2018, Zone 1 switchgrass yields tended to be greater than in Zone 3. The overall yields were similar, if not slightly better than the historical yields at our experimental field site.

This thesis adds to the scientific community's knowledge of how to delineate management zone with proximal soil sensing data, and also reveals that N fertilizer rates are not the sole predictor of GHG emissions. This thesis adds to the knowledge of the agronomic decision-making community by demonstrating the use of proximal soil sensing data such as soil ECa and bare soil images to create robust maps for field management.

## References

- Abdalla, M., Jones, M., Smith, P., & Williams, M. (2009). Nitrous oxide fluxes and denitrification sensitivity to temperature in Irish pasture soils. *Soil Use and Management*, 25, 376-388. <https://doi.org/10.1111/j.1475-2743.2009.00237.x>
- Anderson-Teixeira, K. A., Davis, S. C., Masters, M. D., & Deluca, E. H. (2009). Changes in soil organic carbon under biofuel crops. *GCB Bioenergy*, 1, 75-96. <https://doi.org/10.1111/j.1757-1707.2008.01001.x>
- Banning, N. C., Maccarone, L. D., Fisk, L. M., & Murphy, D. V. (2015) Ammonia-oxidizing bacteria not archaea dominate nitrification activity in semi-arid agricultural soil. *Scientific Reports*, 5, 11146. <https://doi.org/10.1038/srep11146>
- Bouwman, A. F., Boumans, L. J. M., & Bates, N. H. (2002) Emissions of N<sub>2</sub>O and NO from fertilized fields. *Global Biogeochemical Cycles*, 16(4), 1058. <https://doi.org/10.1029/2001GB001811>
- Brahmaprakash, G. P., Sahu, P. K., Lavanya, G., Nair, S. S., Gangaraddi, V. K., & Gupta, A. (2017). Microbial Functions of the Rhizosphere. In D. Singh et al. (Eds.), *Plant-Microbe Interactions in Agro-Ecological Perspectives* (pp. 177-210). Springer, Singapore. [https://doi.org/10.1007/978-981-10-5813-4\\_10](https://doi.org/10.1007/978-981-10-5813-4_10)
- Carey, C. J., Dove, N. C., Beman, J. M., Hart, S. C., & Aronson, E. I. (2016). Meta-analysis reveals ammonia-oxidizing bacteria respond more strongly to nitrogen addition than ammonia-oxidizing archaea. *Soil Biology & Biochemistry*, 99, 158-166. <https://doi.org/10.1016/j.soilbio.2016.05.014>

- Chen, F., Kissel, D. E., West, L. T., & Adkins, W. (2000). Field-scale mapping of surface soil organic carbon using remotely sensed imagery. *Soil Science Society of America Journal*, *64*(2), 746–753. <https://doi.org/10.2136/sssaj2000.642746x>
- Chen, G., Zhu, H., & Zhan, Y. (2008). Soil microbial activities and carbon and nitrogen fixation. *Research in Microbiology*, *154*(5), 393-398. [https://doi.org/10.1016/S0923-2508\(03\)00082-2](https://doi.org/10.1016/S0923-2508(03)00082-2)
- Conen, F., Dobbie, K. E., & Smith, K. A. (2000). Predicting N<sub>2</sub>O emissions from agricultural land through related soil parameters. *Global Change Biology*, *6*(4), 417-426. <https://doi.org/10.1046/j.1365-2486.2000.00319.x>
- Cui, P., Fan, F., Yin, C., Li, Z., Song, A., Wan, Y., & Liang, Y. (2013). Urea- and nitrapyrin-affected N<sub>2</sub>O emission is coupled mainly with ammonia oxidizing bacteria growth in microcosms of three typical Chinese arable soils. *Soil Biology & Biochemistry*, *66*, 214-221. <http://doi.org/10.1016/j.soilbio.2013.08.001>
- FAO, & ITPS. (2015). Status of the world's soil resources (SWSR)-technical summary. Food and Agriculture Organization of the United Nations and Intergovernmental technical Panel on Soils.
- Fisher, K. A., Meisinger, J. J., & James, B. R. (2016) Urea hydrolysis rate in soil toposequences as influenced by pH, carbon, nitrogen, and soluble metals. *Journal of Environmental Quality*, *45*, 349-359. <https://doi.org/10.2134/jeq2015.05.0228>
- Fleming, K. L., Heermann, D. F., & Westfall, D. G. (2004). Evaluating soil color with farmer input and apparent soil electrical conductivity for management zone delineation. *Agronomy Journal*, *96*(6), 1581–1587. <https://doi.org/10.2134/agronj2004.1581>

- Florinsky, I. V., McMahon, S. & Burton, D. L. (2004). Topographic control of soil microbial activity: a case study of denitrifiers. *Geoderma*, 119, 33-53.  
[doi:https://doi.org/10.1016/S0016-7061\(03\)00224-6](https://doi.org/10.1016/S0016-7061(03)00224-6).
- Frank, S., Beach, R., Havlík, P., Valin, H., Herrero, M., Mosnier, A., Hasegawa, T., Creason, J., Ragnauth, S., & Obersteiner, M. (2018). Structural change as a key component for agricultural non-CO<sub>2</sub> mitigation efforts. *Nature Communications*, 9, 1060.  
<https://doi.org/10.1038/s41467-018-03489-1>
- Fridgen, J. J., Kitchen, N. R., Sudduth, K. A., Drummond, S. T., Wiebold, W. J., & Fraisse, C. W. (2004). Management Zone Analyst (MZA): Software for subfield management zone delineation. *Agronomy Journal*, 96, 100-108.
- Georgi, C., Spengler, D., Itzerott, S., & Kleinschmit, B. (2018). Automatic delineation algorithm for site-specific management zones based on satellite remote sensing data. *Precision Agriculture*, 19(4), 684–707. <https://doi.org/10.1007/s11119-017-9549-y>
- Gernaat, D. E. H. J., Calvin, K., Lucas, L. L., Luderer, G., Otto, S. A. C., Rao, S., Strefler, J., & van Vuuren, D. P. (2015). Understanding the contribution of non-carbon dioxide gases in deep mitigation scenarios. *Global Environmental Change*, 33, 142-153.  
<https://doi.org/10.1016/j.gloenvcha.2015.04.010>
- Hayatsu, M., Tago, K., & Saito, M. (2008). Various players in the nitrogen cycle: Diversity and functions of the microorganisms involved in nitrification and denitrification. *Soil Science and Plant Nutrition*, 54, 33-45. <https://doi.org/10.1111/j.1747-0765.2007.00195.x>.

- Iqbal, J., Ronggui, H., Lijun, D., Lan, L., Shan, L., Tao, C., & Leilei, R. (2008). Differences in soil CO<sub>2</sub> flux between different land use types in mid-subtropical China. *Soil Biology and Biochemistry*, 40, 2324-2333. <https://doi.org/10.1016/j.soilbio.2008.05.010>
- Kiss, S., & Simhaian, M. (2002). *Improving efficiency of urea fertilizers by inhibition of soil urease activity*. Kluwer Academic Publishers.
- Kool, D. K., Dolfing, J., Wrage, N., & Van Groenigen, J. W. (2011). Nitrifier denitrification as a distinct and significant source of nitrous oxide from soil. *Soil Biology & Biochemistry*, 43, 174-178. <https://doi.org/10.1016/j.soilbio.2010.09.030>
- Kunhikrishnan, A., R. Thangarajan, R., Bolan, N. S., Xu, Y., Mandal, S., Gleeson, D. B., Seshadri, B., Zaman, M., Barton, L., Tang, C., Luo, J., Dalal, R., Ding, W., Kirkham, M. B., & Naidu, R. (2016). Chapter One - Functional Relationships of Soil Acidification, Liming, and Greenhouse Gas Flux. In D. L. Sparks (Ed.), *Advances in Agronomy* (pp. 1-71). Academic Press. <https://doi.org/10.1016/bs.agron.2016.05.001>
- Li, Y., Chapman, S. J., Nicol, G. W., & Yao, H. (2018). Nitrification and nitrifiers in acidic soils. *Soil Biology & Biochemistry*, 116, 290-301. <https://doi.org/10.1016/j.soilbio.2017.10.023>
- Longchamps, L., & Khosla, R. (2017). Precision maize cultivation techniques. In D. Watson (Ed.), *Achieving sustainable cultivation of maize: Cultivation techniques, pest and disease control*. 107–148. Burleigh Dodds Science Publishing.
- Martel, H., & Lalonde, O. (2018). Guide de Production Panic Erige. Guide de Production Panic Erige. Réseau des plantes bio-industrielles du Québec.

- McDaniel, M. D., Simpson, R. R., Malone, B. P., McBratney, A. B., Minasny, B., & Adams, M. A. (2017). Quantifying and predicting spatio-temporal variability of soil CH<sub>4</sub> and N<sub>2</sub>O fluxes from a seemingly homogeneous Australian agricultural field. *Agriculture, Ecosystems & Environment*, *240*, 182-193. doi:  
<https://doi.org/10.1016/j.agee.2017.02.017>
- Meinhardt, K. A., Stopnisek, N., Pannu, M. W., Strand, S. E., Fransen, S. C., Casciotti, K. L., & Stahl, D. A. (2018). Ammonia-oxidizing bacteria are the primary N<sub>2</sub>O producers in an ammonia-oxidizing archaea dominated alkaline agricultural soil. *Environmental Microbiology*, *20*(6), 2195-2206. <https://doi.org/10.1111/1462-2920.14246>
- Merbt, S. N., Proia, L., Prosser, J. L., Marti, E., Casamayor, E. O., & von Schiller, D. (2016). Stream drying drive microbial ammonia oxidation and first-flush nitrate export. *Ecology*, *97*(9), 2192-2198. <https://doi.org/10.1002/ecy.1486>
- Monti, A., Barbanti, L., Zatta, A., & Zegada-Lizarazu, W. (2012). The contribution of switchgrass in reducing GHG emissions. *GCB Bioenergy*, *4*, 420-434.  
<https://doi.org/10.1111/j.1757-1707.2011.01142.x>
- Moral, F. J., & Serrano, J. M. (2019). Using low-cost geophysical survey to map soil properties and delineate management zones on grazed permanent pastures. *Precision Agriculture*, *20*, 1000–1014. <https://doi.org/10.1007/s11119-018-09631-9>
- Munch, C. J., & Velthof, G. L. (2007). Chapter 21 - Denitrification and Agriculture A2 - Bothe, Hermann. In: S. J. Ferguson & W. E. Newton (Eds.), *Biology of the Nitrogen Cycle* (pp. 331-341). Elsevier, Amsterdam.

- Okibe, S. T., Augustin, J., Mansour, I., & Veresoglou, S. D. (2019). Disentangling direct and indirect effects of mycorrhiza on nitrous oxide activity and denitrification. *Soil Biology & Biochemistry*, *134*, 142-151. <https://doi.org/10.1016/j.soilbio.2019.03.025>
- Scholefield, D., Hawkins, J. M. B., & Jackson, S. M. (1997). Development of a helium atmosphere soil incubation technique for direct measurement of nitrous oxide and dinitrogen fluxes during denitrification. *Soil Biology & Biochemistry*, *29*(9-10), 1345-1352. [https://doi.org/10.1016/S0038-0717\(97\)00021-7](https://doi.org/10.1016/S0038-0717(97)00021-7)
- Seitzinger, S., Harrison, J. A., Böhlke, J. K., Bouwman, A. F., Lowrance, R., Peterson, B., Tobias, C., & Van Drecht, G. (2006). Denitrification across landscapes and waterscapes: A synthesis. *Ecological Applications*, *16*(6), 2064-2090.
- Shah, T., Lateef, S., & Noor, M. A. (2020). Carbon and nitrogen cycling in agroecosystems: An overview. In R. Datta et al. (Eds.), *Carbon and nitrogen cycling in soil* (pp. 1-15). Springer Nature Singapore Pte Ltd.
- Sharkey, T. D., Ducruet, J.-M., & Parry, M. A. J. (2012). Biochemistry and photochemistry of terrestrial photosynthesis: a synopsis. In J. Flexas et al. (Eds.), *Terrestrial photosynthesis in a changing environment: A molecular, physiological and ecological approach* (pp. 9-19). Cambridge University Press.
- Shen, Y., Sui, P., Huang, J., Wang, D., Whalen, J. K., & Chen, Y. (2018). Greenhouse gas emissions from soil under maize-soybean intercrop in the North China Plain. *Nutrient Cycling in Agroecosystems*, *110*, 451-465. <https://doi.org/10.1007/s10705-018-9908-8>

- Shi, X., Hu, H.-W., Zhu-Barker, X., Hayden, H., Wang, J., Suter, H., Chen, D., & He, J.-Z. (2017). Nitrifier-induced denitrification is an important source of soil nitrous oxide and can be inhibited by a nitrification inhibitor 3,4-dimethylpyrazole phosphate. *Environmental Microbiology*, *19*(12), 4851-4865. <https://doi.org/10.1111/1462-2920.13872>
- Weismeyer, M., Urbanski, L., Hobley, E., Lang, B., von Lützowa, M., Marin-Spiotta, E., van Wesemael, B., Rabot, E., Ließ, M., Gracia-Franco, N., Wollschläger, U., Vogelf, H.-J., & Kögel-Knabner, I. (2019). Soil organic carbon storage as key function of soils – A review of drivers and indicators at various scales. *Geoderma*, *333*, 149-162. <https://doi.org/10.1016/j.geoderma.2018.07.026>
- Whalen, J.K., & Sampedro, L. (2010). *Soil Ecology and Management*. CABI.
- Wile, A., Burton, D. L., Sharifi, M., Lynch, D., Main, M., & Papadopoulos, Y. A. (2014). Effect of nitrogen fertilizer application rate on yield, methane and nitrous oxide emissions from switchgrass (*Panicum virgatum* L.) and reed canarygrass (*Phalaris arundinacea* L.). *Canadian Journal of Soil Science*, *94*, 129-137. <https://doi.org/10.4141/CJSS2013-058>
- Wrage-Mönnig, N., Horn, M. A., Well, R., Müller, C., Velthof, G., & Oenema, O. (2018). The role of nitrifier denitrification in the production of nitrous oxide revisited. *Soil Biology & Biochemistry*, *123*, A3-A16. <https://doi.org/10.1016/j.soilbio.2018.03.020>
- Xiang, X., He, D., He, J.-S., Myrold, D. D., & Chu, H. (2017). Ammonia-oxidizing bacteria rather than archaea respond to short-term urea amendment in an alpine grassland, *Soil Biology and Biochemistry*, *107*, 218-225. <https://doi.org/10.1016/j.soilbio.2017.01.012>

- Yao, P., Li, X., Nan, W., Li, X., Zhang, H., Shen, Y., Li, S., & Yue, S. (2017). Carbon dioxide fluxes in soil profiles as affected by maize phenology and nitrogen fertilization in the semiarid Loess Plateau. *Agriculture, Ecosystems & Environment*, 236, 120-133.  
<https://doi.org/10.1016/j.agee.2016.11.020>.
- Yari, A., Madramootoo, C. A., Woods, S. A., Adamchuk, V., & Huang, H. H. (2017). Assessment of field spatial and temporal variabilities to delineate site-specific management zones for variable-rate irrigation. *Journal of Irrigation and Drainage Engineering*, 143(9), 04017037. [https://doi.org/10.1061/\(ASCE\)IR.1943-4774.0001222](https://doi.org/10.1061/(ASCE)IR.1943-4774.0001222)
- Zou, W., Ji, W., Si, B. C., & Biswas, A. (2018). Detecting nonlinearity in the spatial series of nitrous oxide emission by delay vector variance. *Geoderma*, 317, 23-31.  
<https://doi.org/10.1016/j.geoderma.2017.12.023>